LIPSCHITZ STABILITY FOR BACKWARD HEAT EQUATION WITH APPLICATION TO FLUORESCENCE MICROSCOPY*

PABLO ARRATIA†, MATÍAS COURDURIER‡, EVELYN CUEVA§, AXEL OSSES¶, AND BENJAMÍN PALACIOS‖

Abstract. In this work we study a Lipschitz stability result in the reconstruction of a compactly supported initial temperature for the heat equation in $\mathbb{R}^n$, from measurements along a positive time interval and over an open set containing its support. We take advantage of the explicit dependency of solutions to the heat equation with respect to the initial condition. By means of Carleman estimates we obtain an analogous result for the case when the observation is made along an exterior region $\omega \times (\tau, T)$, such that the unobserved part $\mathbb{R}^n \backslash \omega$ is bounded. In the latter setting, the method of Carleman estimates gives a general conditional logarithmic stability result when initial temperatures belong to a certain admissible set, and without the assumption of compactness of support. Furthermore, we apply these results to deduce a similar result for the heat equation in $\mathbb{R}$ for measurements available on a curve contained in $\mathbb{R} \times [0, \infty)$, from where a stability estimate for an inverse problem arising in 2D Fluorescence Microscopy is deduced as well. In order to further understand this Lipschitz stability, in particular, the magnitude of its stability constant with respect to the noise level of the measurements, a numerical reconstruction is presented based on the construction of a linear system for the inverse problem in Fluorescence Microscopy. We investigate the stability constant with the condition number of the corresponding matrix.

Key words. Backward Heat Equation, Lipschitz stability, Inverse Problem, Fluorescence Microscopy.

AMS subject classifications. 35B35, 35K05, 35R30.

1. Introduction.

In this paper we consider the heat equation in $\mathbb{R}^n$:

$$
\left\{
\begin{array}{rcll}
u_t - \Delta u & = & 0 & \text{in } \mathbb{R}^n \times (0, T), \\
u(y, 0) & = & u_0(y) & \text{in } \mathbb{R}^n, \\
\lim\limits_{|y| \to \infty} u(y, t) & = & 0 & t \in (0, T).
\end{array}
\right. \tag{1.1}
$$

We are interested in the reconstruction of the initial temperature u_0 when measurements are available in a certain open region. This problem is known as the backward heat equation inverse problem and is an ill-posed problem in the sense of Hadamard [10], *i.e.*, small noise on observations may cause large errors in the reconstruction of the initial condition. Ill-posedness may be overcome by incorporating a priori information about the solutions. A common hypothesis that frequently appears in the literature consists in assuming that the initial condition belongs to a bounded set of some Sobolev space [7, 12, 15, 23, 24]. This approach is taken into account in order to deduce a conditional logarithmic stability when measurements are made on $\omega \times (\tau, T)$,

*Submitted to the editors DATE.

Funding: This work was funded by ANID-Fondecyt grants #1191903 and #1201311, Basal Program CMM-AFB 170001, FONDAP/15110009.

†Departamento de Ingeniería Matemática, FCFM, Universidad de Chile, Chile (parratia@dim.uchile.cl).

‡Facultad de Ciencias Matemáticas, Pontificia Universidad Católica de Chile, Chile (mcourdurier@mat.uc.cl).

§Research Center on Mathematical Modeling (MODEMAT), Escuela Politécnica Nacional, Quito, Ecuador (ecueva@dim.uchile.cl).

¶Departamento de Ingeniería Matemática and Centro de Modelamiento Matemático, UMI CNRS 2807, FCFM, Universidad de Chile, Chile (axosses@dim.uchile.cl).

‖Department of Statistics, University of Chicago, US (bpalacios@uchicago.edu).

for $0 \le \tau < T$ and ω an open set with bounded complement. Namely, given $\beta > 0$ and $M > 0$, we consider the following admissible set:

$$\mathcal{A}_{\beta,M} := \{a \in H^{2\beta}(\mathbb{R}^n) : ||a||_{H^{2\beta}(\mathbb{R}^n)} \le M\}. \tag{1.2}$$

The conditional logarithmic stability is stated as follows:

THEOREM 1.1. *Let u be a solution of (1.1) with $u_0 \in \mathcal{A}_{\beta,M}$. Let $\omega \times (\tau, T)$ be the observation region where $0 \le \tau < T$ and $\omega \subseteq \mathbb{R}^n$ is an open set such that $\mathbb{R}^n \backslash \omega$ is compact. Let us suppose that $||u||_{L^2(\omega\times(\tau,T))} < 1$. Then, there exist constants $\kappa \in (0, 1)$ and $C_1 = C_1(M, \beta, \tau, T, \omega) > 0$ such that*

$$||u_0||_{L^2(\mathbb{R}^n)} \le C_1(-\log ||u||_{L^2(\omega\times(\tau,T))})^{-\kappa}.$$

To conclude this result, we use a Carleman inequality obtained in [13]. The main problem is that the inequality established in [13] does not hold for unbounded domains such as $\mathbb{R}^n$. In order to be able to apply the Carleman estimate, we use some ideas taken from [3], where null controllability for the heat equation is proved for a control region with bounded complement. Such a large region of control seems to be necessary, as shown in [17, 18].

The main result of this paper is in the context of compactly supported initial conditions, where the above logarithmic inequality can be improved to a Lipschitz one. The precise result is stated in Theorem 1.2 below. It is in fact a consequence of an analogous result, Theorem 1.3, for the closely related inverse problem of backward heat propagation with observation in an open region surrounding the support of the initial heat profile.

THEOREM 1.2. *For $R > 0$ we define $B := B(0, R)$ the ball of radius R and centered at the origin. Let $0 \le \tau < T$ and $\omega \subseteq \mathbb{R}^n$ be such that $\mathbb{R}^n \backslash \omega$ is compact and $B \subseteq \mathbb{R}^n \backslash \omega$. Let $u_0 \in L^1(\mathbb{R}^n)$ be with $\mathrm{supp}(u_0) \subseteq B$ and u be the respective solution of (1.1). Then there exists a constant $C_2 = C_2(R, \tau, T, \omega) > 0$ such that*

$$||u_0||_{L^1(\mathbb{R}^n)} \le C_2||u||_{L^2(\omega\times(\tau,T))}.$$

THEOREM 1.3. *Let B be as before. If $u_0 \in L^1(\mathbb{R}^n)$ with $\mathrm{supp}(u_0) \subseteq B$, then there exists a constant $C_3 = C_3(R, t_1, t_2) > 0$, for $0 < t_1 < t_2$, such that*

$$||u_0||_{L^1(\mathbb{R}^n)} \le C_3||u||_{L^2(2B\times(t_1,t_2))}.$$

Theorem 1.3 states that we can get an estimate of the initial condition u_0 with respect to observations made on an open set containing the support of u_0 and for times in a positive interval, while Theorem 1.2 states the analogous result for exterior measurements. To the best of our knowledge, few results about Lipschitz stability for backward heat equation exist in the literature. In [24], a similar estimate is obtained for the reconstruction of the solution at a positive time $t > 0$ and measurements acquired on a subdomain, while in [20], a Lipschitz stability estimate is obtained for the problem of reconstructing the initial condition, although with a very strong norm associated to the (boundary) observations that involve the use of time derivatives of all orders. In our case, we exploit the explicit dependency on the heat equation solution in all of $\mathbb{R}^n$ with respect to the initial condition, as the convolution with the heat kernel.

The study of the backward heat equation with compactly supported initial conditions arises from an inverse problem related to the microscopy technique performed by a Light Sheet Fluorescence Microscope (LSFM) [9, 11, 14]. Images obtained from this kind of microscopes present undesirable properties such as blurring and calibration problems so that, in order to improve the final images, a mathematical direct model was established in [6] with the aim of characterizing and analyzing the imaging modality as an inverse problem. Such approach is applied to the imaging of two dimensional specimens, where the light sheet illumination reduces to a laser beam emitted at different heights y. The fluorescent distribution is denoted by μ and is the physical quantity to be reconstructed. At the end of the process, the measurement $p(s, y)$ obtained at pixel s of the camera for the illumination at height $y \in Y_s$ is given by the following expression:

(1.3)
$$p(s,y) = c \cdot \exp\left(-\int_{\gamma(y)}^{s} \lambda(\tau,y)d\tau\right) \int_{\mathbb{R}} \frac{\mu(s,r)e^{-\int_r^\infty a(s,\tau)d\tau}}{\sqrt{4\pi\sigma(s,y)}} \exp\left(-\frac{(r-h)^2}{4\sigma(s,y)}\right) dr,$$

where
$$\sigma(s,y) = \frac{1}{2}\int_{\gamma(y)}^{s} (s-\tau)^2 \psi(\tau,y)d\tau.$$

Here, λ, a and ψ are physical parameters related with attenuation or scattering and γ is a function related with the geometry of Ω, more specifically, $\gamma(y)$ is defined such that $(\gamma(y), y)$ is the first point at height y belonging to $\partial\Omega$. These and other terms shall be presented in detail in section 5.

If we fix pixel s and take
$$u_0(y) := \mu(s,y)e^{-\int_y^\infty a(s,\tau)d\tau},$$

the solution u of (1.1) with $n = 1$ evaluated in $(y, \sigma(s, y))$ gives us the measurement obtained by the camera at the pixel s for an illumination made at height y. Furthermore, μ is compactly supported, hence $\mu(s, \cdot)$ is as well. The relation between measurements and u is given by the next expression:

$$\begin{aligned} & p(s,y) = c \cdot \exp\left(-\int_{\gamma(y)}^{s} \lambda(\tau,y)d\tau\right) u(y,\sigma(s,y)) \\ \iff \quad & u(y,\sigma(s,y)) = \frac{1}{c}\exp\left(\int_{\gamma(y)}^{s} \lambda(\tau,y)d\tau\right) p(s,y). \end{aligned}$$

This tells us that if we know physical the parameters λ, ψ and a, then we have access to measurements of u along the curve $\Gamma = \{(y, \sigma(s, y)) : y \in Y_s\} \subseteq \mathbb{R} \times (0, T)$. Consequently, the inverse problem consists in the recovery of the initial temperature from these observations.

Uniqueness has been proved in [6] based on classical unique continuation results for parabolic equations. In this paper we also study the Lipschitz stability in the reconstruction of the fluorescence source μ from measurements available on Γ. This result will be a direct consequence of the following theorem for the reconstruction of the initial temperature from observations made on a curve contained in $\mathbb{R} \times [0, \infty)$, which is constructed as the graph of a function σ that satisfies the following *σ-properties*:

i) $\sigma \in C^1(\mathbb{R})$,
ii) $\sigma > 0$ for $y \in (a_1, a_2)$ and $\sigma(y) \equiv 0$ for $y \in (a_1, a_2)^c$, for some $a_1 < a_2$,

iii) there exists $\xi_1, \xi_2 > 0$ such that $\sigma' > 0$ in $(a_1, a_1 + \xi_1]$, $\sigma' < 0$ in $[a_2 - \xi_2, a_2)$ and $\sigma(a_1 + \xi_1) = \sigma(a_2 - \xi_2)$,

iv) $\dfrac{1}{\sigma'(y)} = \mathcal{O}\left(\exp\left(\dfrac{1}{\sigma(y)}\right)\right)$ as y goes to a_1^+, a_2^-.

The theorem is stated as follows:

THEOREM 1.4. *Consider $\sigma : \mathbb{R} \to \mathbb{R}_+$ a function satisfying the σ-properties. Let u be the solution of (1.1) with $n = 1$ for some $u_0 \in L^1(\mathbb{R})$ such that* $\mathrm{supp}(u_0) \subset (a_1 + \delta, a_2 - \delta)$*, where $0 < \delta < (a_2 - a_1)/2$. Let $\Gamma_L := \{(y, \sigma(y)) : y \in (-\infty, a_1 + \xi_1]\}$ and $\Gamma_R := \{(y, \sigma(y)) : y \in [a_2 - \xi_2, \infty)\}$ be two curves contained in $\mathbb{R} \times [0, \infty)$ where measurements are available. Then there exists a constant $C_4 = C_4(\sigma, \delta) > 0$ such that*

$$||u_0||_{L^1(\mathbb{R})} \leq C_4 ||u||_{L^1(\Gamma_L \cup \Gamma_R)}$$

Remark 1.5. The mentioned σ-properties, specially the last one, may not be necessary conditions to conclude Theorem 1.4, but are suitable for the LSFM inverse problem.

In particular, this theorem implies uniqueness for the inverse problem. Numerical results are carried out after discretizing (1.3). Notice that measurements are linear with respect to μ, hence we investigate the stability of the LSFM problem by solving a linear system. Moreover, for the matrix associated, we study its condition number in order to appreciate the behavior of the stability constant. At this point we have to be careful: a Lipschitz type stability may be good from the mathematical point of view, but if the constant is too large with respect to noise level measurements, then the numerical reconstruction may not be satisfactory. Finally, we consider what happens with the reconstruction when the physical parameters λ, a and ψ depend on μ, *i.e.*, are also unknown.

The paper is organized as follows: section 2 is devoted to demonstrate Theorem 1.1. There, we introduce Theorem 2.1 to show an energy estimate of u which is used later in section 3 to prove Theorem 1.3. In section 4 we prove Theorem 1.4. Section 5 proves the stability of the 2D LSFM inverse problem. Finally, section 6 studies from the numerical point of view the result obtained for the LSFM problem.

2. Conditional Logarithmic Stability.

As said before, since the backward heat equation inverse problem is a well known ill-posed problem, we use the admissible set $\mathcal{A}_{\beta,M}$ previously defined in (1.2) to add some a priori information on the solution.

To prove Theorem 1.1 let us demonstrate two theorems:

THEOREM 2.1. *Let $0 \leq \tau < T$ and $\omega \subseteq \mathbb{R}^n$ be an open set such that $\mathbb{R}^n \backslash \omega$ is compact. Let u be a solution of (1.1). Then for all $0 < \varepsilon < (T - \tau)/2$ there exists a constant $C_5 = C_5(\varepsilon, \tau, T, \omega) > 0$ such that*

$$||u_t||_{L^2(\tau+\varepsilon, T-\varepsilon; H^{-1}(\mathbb{R}^n))} + ||u||_{L^2(\tau+\varepsilon, T-\varepsilon; H^1(\mathbb{R}^n))} \leq C_5 ||u||_{L^2(\tau, T; L^2(\omega))}.$$

Remark 2.2. The above result holds true even for $\tau = 0$ but the constant C_5 tends to ∞ as ε tends to 0.

Remark 2.3. Theorem 2.1 holds true also after replacing $\mathbb{R}^n$ by an unbounded domain Ω of class C^2 uniformly. This could help to extend the logarithmic stability to a more general unbounded set (not only $\mathbb{R}^n$), however, Theorem 2.5 below fails when dealing with such sets. Hence, the conditional logarithmic stability for a general unbounded set when measurements are made in the region $\omega \times (\tau, T)$ remains an open problem.

Proof of Theorem 2.1. We follow [3] to get an estimate of $||u||_{L^2(\tau+\varepsilon,T-\varepsilon;L^2(\mathbb{R}^n))}$. To estimate $||\nabla u||^2_{L^2(\tau+\varepsilon,T-\varepsilon;L^2(\mathbb{R}^n))}$ we make a slight modification to the same argument to conclude. Finally, $||u_t||_{L^2(\tau+\varepsilon,T-\varepsilon;H^{-1}(\mathbb{R}^n))}$ is directly estimated from the heat equation (1.1). In the points I)-III) presented below, we respectively estimate each one of these terms:

I) Estimation of $||u||_{L^2(\tau+\varepsilon,T-\varepsilon;L^2(\mathbb{R}^n))}$. Let $\delta > 0$ small enough. Without loss of generality we may assume that $\mathbb{R}^n\backslash\omega$ is connected. Then, we define a cut-off function $\rho \in C^\infty(\mathbb{R}^n)$ as follows:

$$\begin{cases} \rho = 1 & \text{in } \mathbb{R}^n\backslash\omega \\ \rho = 0 & \text{in } \omega_\delta := \{x \in \omega : d(x, \partial\omega) > \delta\} \\ \rho \in (0,1] & \text{in } \omega\backslash\omega_\delta. \end{cases}$$

The aim of this function is to localize the solution in the bounded set where observations are not available. Consider $\theta = \rho u$ and let $\Theta = \{x \in \mathbb{R}^n : \rho(x) > 0\}$. Notice that $\theta = 0$ in $\mathbb{R}^n\backslash\Theta$ and since u satisfies (1.1), then θ satisfies the following parabolic equation in a bounded domain:

$$\begin{cases} \theta_t - \Delta\theta = g & \text{in } \Theta \times (0,T) \\ \theta = 0 & \text{on } \partial\Theta \times (0,T) \\ \theta(x,0) = \rho u_0(x) & \text{in } \Theta, \end{cases} \tag{2.1}$$

where $g = -\Delta\rho u - 2\nabla\rho \cdot \nabla u$. Since Θ is bounded, we can apply the Carleman estimate shown in [13] with $l = 1$. More precisely, let ν be defined as below (we refer to [4], lemma 1.1, for the existence of such function):

$$\begin{cases} \nu \in C^2(\bar{\Theta}) \\ \nu > 0 \text{ in } \Theta,\ \nu = 0 \text{ on } \partial\Theta \\ \nabla\nu \neq 0 \text{ in } \overline{\Theta\backslash\omega} \end{cases}$$

and consider the following Carleman weights:

$$\xi(x,t) = \frac{e^{\lambda\nu(x)}}{(t-\tau)(T-t)}, \quad \zeta(x,t) = \frac{e^{\lambda\nu(x)} - e^{2\lambda||\nu(x)||_{C(\overline{\Theta})}}}{(t-\tau)(T-t)}. \tag{2.2}$$

Thus, from [13] we know that the next Carleman estimate holds: there exists $\hat{\lambda} > 0$ such that for an arbitrary $\lambda \geq \hat{\lambda}$ there exists $s_0(\lambda)$ and a constant $C > 0$ satisfying

$$\begin{aligned} &\int_\tau^T \int_\Theta \left(\frac{1}{s\xi}|\nabla\theta|^2 + s\xi|\theta|^2\right) e^{2s\zeta} dxdt \\ &\leq C\left(||ge^{s\zeta}||^2_{L^2(\tau,T;H^{-1}(\Theta))} + \int_\tau^T \int_{\Theta\cap\omega} s\xi|\theta|^2 e^{2s\zeta} dxdt\right) \quad \forall s \geq s_0(\lambda), \end{aligned} \tag{2.3}$$

where θ is the solution of (2.1). Let us estimate the terms in the right and left hand sides of (2.3):

- Recall that $g = -\Delta\rho u - 2\nabla\rho \cdot \nabla u$. Noticing that $\Delta\rho = 0$ in $\Theta\backslash\omega$ and $e^{s\zeta} < 1$ (since $\zeta < 0$), the first term is directly estimated as follows

$$||\Delta\rho u e^{s\zeta}||^2_{L^2(\tau,T;H^{-1}(\Theta))} \leq C||u||^2_{L^2((\tau,T)\times\omega)},$$

where the constant $C > 0$ depends on ρ. For the second term, we notice that

$$-2(\nabla\rho \cdot \nabla u)e^{s\zeta} = -2\nabla \cdot (ue^{s\zeta}\nabla\rho) + 2ue^{s\zeta}\Delta\rho + 2use^{s\zeta}\nabla\rho \cdot \nabla\zeta.$$

Again, $\nabla\rho = 0$, $\Delta\rho = 0$ in $\Theta\backslash\omega$, $e^{s\zeta} < 1$. Besides, noticing that there exists $s_1 > 0$ such that $\left|se^{s\zeta}\dfrac{\partial\zeta}{\partial x_i}\right| < 1$, $\forall i \in \{1, \dots, n\}$, we have that

$$||2(\nabla\rho \cdot \nabla u)e^{s\zeta}||^2_{L^2(\tau,T;H^{-1}(\Theta))} \leq C||u||^2_{L^2(\tau,T;L^2(\omega))}, \quad \forall s \geq s_1.$$

The constant $C > 0$ depends on ρ. Finally, we conclude that

$$||ge^{s\zeta}||^2_{L^2(\tau,T;H^{-1}(\Theta))} \leq C||u||^2_{L^2((\tau,T)\times\omega)}, \quad \forall s \geq s_1. \tag{2.4}$$

- We define the functions $\hat{\xi}$, $\hat{\zeta}$ as in (2.2) but with $\lambda = \hat{\lambda}$. Since $\nu \in C^2(\overline{\Theta})$ there exist constants $\eta_1, \eta_2 > 0$ such that

$$\frac{\eta_1}{(t-\tau)(T-t)} \leq \hat{\xi} \leq \frac{\eta_2}{(t-\tau)(T-t)}.$$

Finally, let $\hat{s} := \max\{s_0(\hat{\lambda}), s_1\}$. Inequality (2.3) leads to

$$\begin{aligned}&\int_\tau^T \int_\Theta \left(\frac{(t-\tau)(T-t)}{\hat{s}}|\nabla\theta|^2 + \frac{\hat{s}}{(t-\tau)(T-t)}|\theta|^2\right) e^{2\hat{s}\hat{\zeta}} dxdt \\ &\leq C\left(||u||^2_{L^2((\tau,T)\times\omega)} + \int_\tau^T \int_{\Theta\cap\omega} \frac{\hat{s}}{(t-\tau)(T-t)}|\theta|^2 e^{2\hat{s}\hat{\zeta}} dxdt\right).\end{aligned} \tag{2.5}$$

We now estimate the weights in (2.5) using the following lemma from [3]:

Lemma 2.4. *Let k, K be two positive constants such that*

$$k \leq e^{2\hat{\lambda}||\nu||_{C(\Theta)}} - e^{\hat{\lambda}\nu(x)} \leq K, \quad x \in \overline{\Theta}.$$

Then, for $x \in \overline{\Theta}$ and $0 < \varepsilon < (T-\tau)/2$ we have

$$\left|\left|\frac{\hat{s}}{(t-\tau)(T-t)}e^{2\hat{s}\hat{\zeta}}\right|\right|_{L^\infty((\Theta\cap\omega)\times(\tau,T))} \leq \frac{1}{2k}e^{-1},$$

$$\frac{(t-\tau)(T-t)}{\hat{s}}e^{2\hat{s}\hat{\zeta}} \geq \frac{\varepsilon(T-\tau-\varepsilon)}{\hat{s}}\exp\left(\frac{-2\hat{s}K}{\varepsilon(T-\tau-\varepsilon)}\right), \quad t \in [\tau+\varepsilon, T-\varepsilon].$$

From this lemma, the left-hand side in (2.5) takes the form

$$\begin{aligned}&\int_\tau^T \int_\Theta \left(\frac{(t-\tau)(T-t)}{\hat{s}}|\nabla\theta|^2 + \frac{\hat{s}}{(t-\tau)(T-t)}|\theta|^2\right) e^{2\hat{s}\hat{\zeta}} dxdt \\ &\qquad \geq \int_{\tau+\varepsilon}^{T-\varepsilon} \int_\Theta \frac{(t-\tau)(T-t)}{\hat{s}}|\nabla\theta|^2 e^{2\hat{s}\hat{\zeta}} dxdt \\ &\qquad \geq C(\varepsilon)\int_{\tau+\varepsilon}^{T-\varepsilon} \int_\Theta |\nabla\theta|^2 dxdt,\end{aligned} \tag{2.6}$$

where $C(\varepsilon)$ is the lower bound of the last inequality in Lemma 2.4 and tends to 0 as ε tends to 0. On the other hand, the second term in the right-hand side in (2.5) is estimated as follows:

$$\begin{aligned}\int_\tau^T\int_{\Theta\cap\omega}\frac{\hat{s}}{(t-\tau)(T-t)}|\theta|^2e^{2s\zeta}dxdt &\le \frac{1}{2k}e^{-1}\int_\tau^T\int_{\Theta\cap\omega}|\theta|^2dxdt\\ \text{(since } \rho<1 \text{ in } \Theta\cap\omega) &\le \frac{1}{2k}e^{-1}\int_\tau^T\int_{\Theta\cap\omega}|u|^2dxdt\\ &\le C||u||^2_{L^2(\tau,T;L^2(\omega))}.\end{aligned}\tag{2.7}$$

Thus, from (2.5), (2.6) and (2.7) we have that

$$\int_{\tau+\varepsilon}^{T-\varepsilon}\int_\Theta|\nabla\theta|^2dxdt\le\frac{C}{C(\varepsilon)}||u||^2_{L^2(\tau,T;L^2(\omega))}.\tag{2.8}$$

Since θ is null on $\partial\Theta$, we use λ_1 the first eigenvalue of $-\Delta$ in $H_0^1(\Theta)$. Furthermore, $\rho=1$ in $\mathbb{R}^n\backslash\omega$, hence

$$\lambda_1\int_{\tau+\varepsilon}^{T-\varepsilon}\int_{\mathbb{R}^n\backslash\omega}|u|^2dxdt=\lambda_1\int_{\tau+\varepsilon}^{T-\varepsilon}\int_{\mathbb{R}^n\backslash\omega}|\theta|^2dxdt\le\int_{\tau+\varepsilon}^{T-\varepsilon}\int_\Theta|\nabla\theta|^2dxdt.$$

Hence we conclude that

$$||u||^2_{L^2(\tau+\varepsilon,T-\varepsilon;L^2(\mathbb{R}^n))}\le\frac{C}{\lambda_1C(\varepsilon)}||u||^2_{L^2((\tau,T)\times\omega)}.\tag{2.9}$$

II) Estimation of $||\nabla u||_{L^2(\tau+\varepsilon,T-\varepsilon;L^2(\mathbb{R}^n))}$. We focus on the second inequality in Lemma 2.4 but for $t\in[\tau+\varepsilon/2,T-\varepsilon]$. When t is in the latter interval we have the following estimate:

$$\frac{(t-\tau)(T-t)}{\hat{s}}e^{2\hat{s}\hat{\varsigma}}\ge\frac{\varepsilon/2(T-\tau-\varepsilon/2)}{\hat{s}}\exp\left(\frac{-2\hat{s}K}{\varepsilon/2(T-\tau-\varepsilon/2)}\right)=:\bar{C}(\varepsilon).$$

Same calculations as in the previous item lead to

$$\int_{\tau+\varepsilon/2}^{T-\varepsilon}\int_{\mathbb{R}^n}|u|^2dxdt\le\frac{C}{\lambda_1\bar{C}(\varepsilon)}||u||^2_{L^2(\tau,T;L^2(\omega))}.\tag{2.10}$$

Let $\chi(t)\in C^\infty([\tau,T])$, with $\chi(t)=0$ for $t\in[\tau,\tau+\varepsilon/2]$, $\chi(t)$ strictly increasing in $(\tau+\varepsilon/2,T-\varepsilon)$, and $\chi(t)=1$ in $[T-\varepsilon,T]$. Multiplying the heat equation (1.1) by $u\chi(t)$ and integrating over $\mathbb{R}^n$, we get

$$\int_{\mathbb{R}^n}|\nabla u|^2\chi dx+\frac{1}{2}\frac{d}{dt}\int_{\mathbb{R}^n}u^2\chi dx=\frac{1}{2}\int_{\mathbb{R}^n}u^2\chi_tdx.$$

Now, integrating over $[\tau+\varepsilon/2,t]$:

$$\begin{aligned}\int_{\tau+\varepsilon/2}^t\int_{\mathbb{R}^n}|\nabla u|^2\chi dxdt+\frac{1}{2}\int_{\mathbb{R}^n}\underbrace{u^2(t)\chi(t)}_{\ge0}-\underbrace{u^2(\tau+\varepsilon/2)\chi(\tau+\varepsilon/2)}_{=0,\text{ since }\chi(\tau+\varepsilon/2)=0}dx\\ =\frac{1}{2}\int_{\tau+\varepsilon/2}^t\int_{\mathbb{R}^n}u^2\chi_tdxdt,\end{aligned}$$

therefore

$$\int_{\tau+\varepsilon/2}^{t}\int_{\mathbb{R}^n}|\nabla u|^2\chi dxdt \leq \frac{1}{2}\int_{\tau+\varepsilon}^{t}\int_{\mathbb{R}^n}u^2\chi_t dxdt \leq ||\chi_t||_\infty \int_{\tau+\varepsilon/2}^{T-\varepsilon}\int_{\mathbb{R}^n}u^2dxdt.$$

Evaluating at $t = T-\varepsilon$ and using (2.10) we have

$$\begin{aligned}\int_{\tau+\varepsilon/2}^{T-\varepsilon}\int_{\mathbb{R}^n}|\nabla u|^2\chi dxdt &\leq ||\chi_t||_\infty \int_{\tau+\varepsilon/2}^{T-\varepsilon}\int_{\mathbb{R}^n}u^2dxdt \\ &\leq \frac{C||\chi_t||_\infty}{\lambda_1\bar{C}(\varepsilon)}||u||^2_{L^2(\tau,T;L^2(\omega))}.\end{aligned} \tag{2.11}$$

Since χ is increasing in $(\tau+\varepsilon, T-\varepsilon)$ the left-hand side leads

$$\begin{aligned}\int_{\tau+\varepsilon/2}^{T-\varepsilon}\int_{\mathbb{R}^n}|\nabla u|^2\chi dxdt &\geq \int_{\tau+\varepsilon}^{T-\varepsilon}\int_{\mathbb{R}^n}|\nabla u|^2\chi dxdt \\ &\geq \chi(\tau+\varepsilon)\int_{\tau+\varepsilon}^{T-\varepsilon}\int_{\mathbb{R}^n}|\nabla u|^2dxdt.\end{aligned} \tag{2.12}$$

Bringing (2.11) and (2.12) together we get

$$\int_{\tau+\varepsilon}^{T-\varepsilon}\int_{\mathbb{R}^n}|\nabla u|^2dxdt \leq \frac{C||\chi_t||_\infty}{\bar{C}(\varepsilon)\chi(\tau+\varepsilon)}||u||^2_{L^2(\tau,T;L^2(\omega))}. \tag{2.13}$$

Hence, with (2.9) and (2.13) we conclude:

$$||u||^2_{L^2(\tau+\varepsilon,T-\varepsilon;H^1(\mathbb{R}^n))} \leq C_5||u||^2_{L^2(\omega\times(\tau,T))},$$

where

$$C_5 = \exp\left(\frac{2\hat{s}K}{\varepsilon(T-\tau-\varepsilon)}\right)\max\left\{\frac{C}{\lambda_1\varepsilon(T-\tau-\varepsilon)}, \frac{C}{\lambda_1\varepsilon(T-\tau-\varepsilon/2)}\frac{||\chi_t||_\infty}{\chi(\tau+\varepsilon)}\right\}.$$

III) Estimation of $||u_t||^2_{L^2(\tau+\varepsilon,T-\varepsilon;H^{-1}(\mathbb{R}^n))}$. Multiplying (1.1) by $v\in H^1(\mathbb{R}^n)$ it follows that

$$\int_{\mathbb{R}^n}u_tvdx = -\int_{\mathbb{R}^n}\nabla u\cdot\nabla vdx.$$

Integrating over $(\tau+\varepsilon, T-\varepsilon)$ and using the estimate obtained before we conclude

$$||u_t||^2_{L^2(\tau+\varepsilon,T-\varepsilon;H^{-1}(\mathbb{R}^n))} \leq ||u||^2_{L^2(\tau+\varepsilon,T-\varepsilon;H^1(\mathbb{R}^n))} \leq C_5||u||^2_{L^2(\omega\times(\tau,T))}. \qquad \square$$

In the next theorem we assume that the initial condition belongs to the admissible set $\mathcal{A}_{\beta,M}$ defined in section 1.

THEOREM 2.5. *Let* $0\leq\tau<T$ *and* $\omega\subseteq\mathbb{R}^n$ *be such that* $\mathbb{R}^n\backslash\omega$ *is compact. Let* u *be a solution of* (1.1) *with initial condition* $u_0\in\mathcal{A}_{\beta,M}$. *Then, for every* $\alpha>0$ *and* $0<\varepsilon<(T-\tau)/2$ *there exists a positive constant* $C_6 = C_6(\alpha,\varepsilon,\tau,T,\omega)$ *such that*

$$||u||_{C([\tau+\varepsilon,T-\varepsilon];L^2(\mathbb{R}^n))} \leq C_6||u||^{\frac{2\alpha}{2\alpha+1}}_{L^2(\omega\times(\tau,T))}.$$

Remark 2.6. The main consequence of this theorem is a Hölder estimate of the solution u at any time $\tau+\varepsilon\leq t\leq T-\varepsilon$:

$$||u(\cdot,t)||_{L^2(\mathbb{R}^n)} \leq C_6||u||^{\frac{2\alpha}{2\alpha+1}}_{L^2(\omega\times(\tau,T))}.$$

Proof. From Theorem 2.1 there exists a constant $C_5 > 0$ such that

$$||u||_{H^1(\tau+\varepsilon,T-\varepsilon;H^{-1}(\mathbb{R}^n))} \le C_5||u||_{L^2(\omega\times(\tau,T))},$$

and using the Sobolev embedding (see theorem 4.12 in [1]) we conclude that

$$||u||_{C([\tau+\varepsilon,T-\varepsilon];H^{-1}(\mathbb{R}^n))} \le C_5||u||_{L^2(\omega\times(\tau,T))}. \tag{2.14}$$

We now estimate $||u||_{C([\tau+\varepsilon,T-\varepsilon];H^{2\alpha}(\mathbb{R}^n))}$ for some given $\alpha > 0$ and conclude the result by interpolation of Sobolev spaces.

Recall that for $a \in H^{2\alpha}(\mathbb{R}^n)$ we have (see e.g. [19], proposition 3.4)

$$\begin{aligned} ||a||^2_{H^{2\alpha}(\mathbb{R}^n)} &= ||a||^2_{L^2(\mathbb{R}^n)} + |a|^2_{H^{2\alpha}(\mathbb{R}^n)} \\ &\le c(||a||^2_{L^2(\mathbb{R}^n)} + ||(-\Delta)^\alpha a||^2_{L^2(\mathbb{R}^n)}), \end{aligned} \tag{2.15}$$

where $|\cdot|_{H^\alpha(\mathbb{R}^n)}$ is the seminorm of Gagliardo for fractional Sobolev spaces and $c = c(n,\alpha)$ is a positive constant.

Recall also that $u(\cdot,t) = e^{t\Delta}u_0$, where $e^{t\Delta}$ corresponds to the heat semigroup. Let us estimate the term $||(-\Delta)^\alpha u||_{L^2(\mathbb{R}^n)}$ via Fourier. Notice that

$$\mathcal{F}((-\Delta)^\alpha e^{t\Delta}u_0) = |\xi|^{2\alpha}e^{-t|\xi|^2}\hat{u}_0.$$

The function $r \in [0,\infty) \to r^{2\alpha}e^{-tr^2}$ reaches its maximum at $\bar{r} = \sqrt{\frac{\alpha}{t}}$ with value $\dfrac{\alpha^\alpha e^{-\alpha}}{t^\alpha}$, so we conclude that

$$||(-\Delta)^\alpha e^{t\Delta}u_0||_{L^2(\mathbb{R}^n)} = |||\xi|^{2\alpha}e^{-t|\xi|^2}\hat{u}_0||_{L^2(\mathbb{R}^n)} \le \frac{C(\alpha)}{t^\alpha}||u_0||_{L^2(\mathbb{R}^n)}. \tag{2.16}$$

Bringing (2.15) and (2.16) together, and since $u_0 \in \mathcal{A}_{\beta,M}$, we get

$$\begin{aligned} ||u||_{C([\tau+\varepsilon,T-\varepsilon];H^{2\alpha}(\mathbb{R}^n))} &= \sup_{t\in[\tau+\varepsilon,T-\varepsilon]} ||u(\cdot,t)||_{H^{2\alpha}(\mathbb{R}^n)} \\ &\le c \sup_{t\in[\tau+\varepsilon,T-\varepsilon]} \left(||u(\cdot,t)||^2_{L^2(\mathbb{R}^n)} + \frac{C^2(\alpha)}{t^{2\alpha}}||u_0||^2_{L^2(\mathbb{R}^n)}\right)^{1/2} \\ &\le c \sup_{t\in[\tau+\varepsilon,T-\varepsilon]} \left(||u_0||^2_{L^2(\mathbb{R}^n)} + \frac{C^2(\alpha)}{(\tau+\varepsilon)^{2\alpha}}||u_0||^2_{L^2(\mathbb{R}^n)}\right)^{1/2} \\ &\le cM\left(1 + \frac{C^2(\alpha)}{(\tau+\varepsilon)^{2\alpha}}\right)^{1/2}. \end{aligned} \tag{2.17}$$

Finally, we use (2.14) and (2.17), and conclude via interpolation theory (proposition 2.3 [16] and section 2.4.1 in [22] or theorem 4.1 in [5]) taking $s = 0, s_0 = -1, s_1 = 2\alpha$ and $\theta = \frac{2\alpha}{2\alpha+1}$ (so that $s = \theta s_0 + (1-\theta)s_1$):

$$\begin{aligned} ||u||_{C([\tau+\varepsilon,T-\varepsilon];L^2(\mathbb{R}^n))} &\le ||u||^{\frac{2\alpha}{2\alpha+1}}_{C([\tau+\varepsilon,T-\varepsilon];H^{-1}(\mathbb{R}^n))}||u||^{\frac{1}{2\alpha+1}}_{C([\tau+\varepsilon,T-\varepsilon];H^{2\alpha}(R^n))} \\ &\le \underbrace{\left[cM\left(1+\frac{C^2(\alpha)}{(\tau+\varepsilon)^{2\alpha}}\right)^{1/2}\right]^{\frac{1}{2\alpha+1}} C_5^{\frac{2\alpha}{2\alpha+1}}}_{=:C_6} ||u||^{\frac{2\alpha}{2\alpha+1}}_{L^2(\omega\times(\tau,T))}. \end{aligned}$$

∎

Let us now derive the conditional logarithmic stability estimate:

Proof of Theorem 1.1. It suffices to follow steps 2 and 3 in the proof of theorem 2.1 of [15]. First of all, the function $t \to ||u(\cdot,t)||^2_{L^2(\mathbb{R}^n)}$ is log-convex, then, for $0 \leq t \leq \theta$, we note that $t = 0 \cdot (1 - t/\theta) + \theta \cdot (t/\theta)$ is a convex combination, hence

$$||u(\cdot,t)||^2_{L^2(\mathbb{R}^n)} \leq ||u_0||^{2(1-t/\theta)}_{L^2(\mathbb{R}^n)} ||u(\cdot,\theta)||^{2t/\theta}_{L^2(\mathbb{R}^n)} \leq M^{2(1-t/\theta)} ||u(\cdot,\theta)||^{2t/\theta}_{L^2(\mathbb{R}^n)}.$$

Integrating from 0 to θ it yields

$$\begin{aligned} \int_0^\theta ||u(\cdot,t)||^2_{L^2(\mathbb{R}^n)} dt &\leq M^2 \int_0^\theta \left(\frac{||u(\cdot,\theta)||_{L^2(\mathbb{R}^n)}}{M} \right)^{2t/\theta} dt \\ &= \theta \left(\frac{||u(\cdot,\theta)||^2_{L^2(\mathbb{R}^n)} - M^2}{\log(||u(\cdot,\theta)||^2_{L^2(\mathbb{R}^n)}) - \log(M^2)} \right). \end{aligned}$$

Due to the logarithm concavity, the right-hand side of the previous estimate is an increasing function with respect to the term $||u(\cdot,\theta)||_{L^2(\mathbb{R}^n)}$, which together with Theorem 2.5 implies that

$$\int_0^\theta ||u(\cdot,t)||^2_{L^2(\mathbb{R}^n)} dt \leq \theta \left(\frac{C_6^2 ||u||^{\frac{4\alpha}{2\alpha+1}}_{L^2(\omega\times(\tau,T))} - M^2}{\log(C_6^2 ||u||^{\frac{4\alpha}{2\alpha+1}}_{L^2(\omega\times(\tau,T))}) - \log(M^2)} \right).$$

Now we have two cases: $C_6 \leq M$ or $M \leq C_6$. We study the first case, the second one is analogous. If $C_6 \leq M$ then

$$\int_0^\theta ||u(\cdot,t)||^2_{L^2(\mathbb{R}^n)} dt \leq M^2 \theta \left(\frac{\frac{C_6^2}{M^2} ||u||^{\frac{4\alpha}{2\alpha+1}}_{L^2(\omega\times(\tau,T))} - 1}{\log(\frac{C_6^2}{M^2} ||u||^{\frac{4\alpha}{2\alpha+1}}_{L^2(\omega\times(\tau,T))})} \right).$$

The right-hand side is increasing as a function of C_6/M and $C_6/M \leq 1$, hence

$$\int_0^\theta ||u(\cdot,t)||^2_{L^2(\mathbb{R}^n)} dt \leq M^2 \theta \left(\frac{||u||^{\frac{4\alpha}{2\alpha+1}}_{L^2(\omega\times(\tau,T))} - 1}{\log(||u||^{\frac{4\alpha}{2\alpha+1}}_{L^2(\omega\times(\tau,T))})} \right).$$

Since measurements are sufficiently small, *i.e.*, $||u||_{L^2(\omega\times(\tau,T))} < 1$, we have that

$$\log ||u||^{\frac{4\alpha}{2\alpha+1}}_{L^2(\omega\times(\tau,T))} < 0,$$

then

$$\int_0^\theta ||u(\cdot,t)||^2_{L^2(\mathbb{R}^n)} dt \leq M^2 \theta \frac{2\alpha+1}{4\alpha} (-\log ||u||_{L^2(\omega\times(\tau,T))})^{-1}.$$

If $M \leq C_6$, we can follow the same steps obtaining that

$$\int_0^\theta ||u(\cdot,t)||^2_{L^2(\mathbb{R}^n)} dt \leq C_6^2 \theta \frac{2\alpha+1}{4\alpha} (-\log ||u||_{L^2(\omega\times(\tau,T))})^{-1}$$

In conclusion, we get the following estimate

$$||u||_{L^2(0,\theta;L^2(\mathbb{R}^n))} \leq \max\{C_6, M\} \left(\theta \frac{2\alpha+1}{4\alpha} \right)^{1/2} (-\log ||u||_{L^2(\omega\times(\tau,T))})^{-1/2}. \tag{2.18}$$

In order to conclude we shall estimate the norms $||u||_{W^{1,p}(0,\theta;L^2(\mathbb{R}^n))}$ and $||u||_{L^p(0,\theta;L^2(\mathbb{R}^n))}$ for some $p>1$ and use interpolation of Sobolev spaces and Sobolev embeddings. On one side we have that

$$u_t(\cdot,t) = \Delta e^{t\Delta}u_0 = -(-\Delta)^{1-\beta}e^{t\Delta}(-\Delta)^{\beta}u_0$$

and thanks to the fractional Laplacian properties (recall (2.16)):

$$||u_t(\cdot,t)||_{L^2(\mathbb{R}^n)} \le \frac{C(\beta)}{t^{(1-\beta)}}||(-\Delta)^{\beta}u_0||_{L^2(\mathbb{R}^n)}.$$

Let $1<p<1/(1-\beta)$. Using that $u_0 \in \mathcal{A}_{\beta,M}$ we get that

$$\begin{aligned}\int_0^\theta ||u_t(\cdot,t)||^p_{L^2(\mathbb{R}^n)}dt &\le C(\beta)\int_0^\theta \frac{1}{t^{p(1-\beta)}}dt\, ||(-\Delta)^\beta u_0||^p_{L^2(\mathbb{R}^n)}\\ &\le C(\beta)\frac{\theta^{1-p(1-\beta)}}{1-p(1-\beta)}\,|u_0|^p_{H^{2\beta}(\mathbb{R}^n)}\\ &\le C(\beta)\frac{\theta^{1-p(1-\beta)}}{1-p(1-\beta)}\,M^p,\end{aligned}$$

that is

$$||u_t||^p_{L^p(0,\theta;L^2(\mathbb{R}^n))} \le C(\beta,M,\theta). \tag{2.19}$$

On the other side,

$$\int_0^\theta ||u(\cdot,t)||^p_{L^2(\mathbb{R}^n)}dt \le \int_0^\theta ||u_0||^p_{L^2(\mathbb{R}^n)}dt \le M^p\theta. \tag{2.20}$$

Bringing (2.19) and (2.20) together we deduce

$$||u||_{W^{1,p}(0,\theta;L^2(\mathbb{R}^n))} \le C(\beta,M,\theta). \tag{2.21}$$

The previous constant decreases with θ, which means that the stability constant decreases when initial time of observation τ is closer to 0. Taking $p\le 2$, we can use (2.18) but with L^p norm in time:

$$||u||_{L^p(0,\theta;L^2(\mathbb{R}^n))} \le \theta^{1/p-1/2}||u||_{L^2(0,\theta;L^2(\mathbb{R}^n))} \le C(-\log||u||_{L^2(\omega\times(\tau,T))})^{-1/2}. \tag{2.22}$$

Again, we interpolate estimates (2.21) and (2.22) so that for $0<s<1$

$$||u||_{W^{1-s,p}(0,\theta;L^2(\mathbb{R}^n))} \le C(-\log||u||_{L^2(\omega\times(\tau,T))})^{-s/2}.$$

Letting s such that $(1-s)p>1$ we can use the Sobolev embedding and conclude with $\kappa = s/2$:

$$||u||_{C([0,\theta];L^2(\mathbb{R}^n))} \le C||u||_{W^{1-s,p}(0,\theta;L^2(\mathbb{R}^n))} \le C_1(-\log||u||_{L^2(\omega\times(\tau,T))})^{-s/2}. \qquad \square$$

3. Conditional Lipschitz Stability. In this section we prove the main results of this paper, Theorem 1.3, which provides a Lipschitz stability inequality in the recovery of the initial condition when observations are made on some interval (t_1,t_2), with $0<t_1<t_2$, and in an open domain containing the support of the initial condition. Theorem 1.2 gives a similar conclusion when measurements are made on an unbounded domain that does not necessarily contain the support of the initial condition. This last theorem follows directly from Theorem 2.1 and Theorem 1.3 and will be used later in section 4.

To demonstrate Theorem 1.3 let us prove first the following lemma whose main hypothesis is that $u_0 \ge 0$:

LEMMA 3.1. *If $u_0 \in L^1(\mathbb{R}^n)$, $u_0 \geq 0$ and $\operatorname{supp}(u_0) \subseteq B := B(0,R)$, for some $R > 0$. Then, for $t > 0$ there exists a constant $C_7 = C_7(R,t) > 0$ such that*

$$||u_0||_{L^1(\mathbb{R}^n)} \leq C_7 ||u(\cdot,t)||_{L^2(2B)}.$$

Proof. We recall that u takes the explicit form

$$u(y,t) = \int_{\mathbb{R}^n} u_0(r) \frac{e^{-\frac{|y-r|^2}{4t}}}{(4\pi t)^{n/2}} dr. \tag{3.1}$$

Since $u_0 \geq 0$ and the heat kernel integrates 1 for any $t > 0$ we have

$$\begin{aligned} ||u_0||_{L^1(\mathbb{R}^n)} = \int_{\mathbb{R}^n} u_0(r) dr &= \int_{\mathbb{R}^n} \int_{\mathbb{R}^n} u_0(r) \frac{e^{-\frac{|y-r|^2}{4t}}}{(4\pi t)^{n/2}} dr dy \\ &= \int_{|y|<2R} \int_{\mathbb{R}^n} u_0(r) \frac{e^{-\frac{|y-r|^2}{4t}}}{(4\pi t)^{n/2}} dr dy \\ &\quad + \int_{|y|>2R} \int_{\mathbb{R}^n} u_0(r) \frac{e^{-\frac{|y-r|^2}{4t}}}{(4\pi t)^{n/2}} dr dy. \end{aligned} \tag{3.2}$$

The first integral on the right hand side is easily bounded by Cauchy-Schwarz and recalling (3.1):

$$\int_{|y|<2R} \int_{\mathbb{R}^n} u_0(r) \frac{e^{-\frac{|y-r|^2}{4t}}}{(4\pi t)^{n/2}} dr dy = \int_{|y|<2R} u(y,t) dy \leq |2B|^{1/2} ||u(\cdot,t)||_{L^2(2B)}, \tag{3.3}$$

where $|2B|$ denotes the volume of the ball of radius $2R$. For the second integral, due to the support of u_0 we notice that

$$\begin{aligned} \int_{|y|>2R} \int_{\mathbb{R}^n} u_0(r) \frac{e^{-\frac{|y-r|^2}{4t}}}{(4\pi t)^{n/2}} dr dy &= \int_{|y|>2R} \int_{|r|<R} u_0(r) \frac{e^{-\frac{|y-r|^2}{4t}}}{(4\pi t)^{n/2}} dr dy \\ &= \int_{|r|<R} u_0(r) \left(\int_{|y|>2R} \frac{e^{-\frac{|y-r|^2}{4t}}}{(4\pi t)^{n/2}} dy \right) dr, \end{aligned}$$

where the integral inside parenthesis can be bounded uniformly with respect to r by a constant $\alpha(R,t) \in (0,1)$, increasing with respect to t. This yields

$$\int_{|y|>2R} \int_{\mathbb{R}^n} u_0(r) \frac{e^{-\frac{|y-r|^2}{4t}}}{(4\pi t)^{n/2}} dr dy \leq \alpha \int_{\mathbb{R}^n} u_0(r) dr. \tag{3.4}$$

Bringing (3.2), (3.3) and (3.4) together we deduce the estimate:

$$||u_0||_{L^1(\mathbb{R}^n)} = \int_{\mathbb{R}^n} u_0(r) dr \leq \underbrace{(1-\alpha)^{-1} C_R}_{=:C_7} ||u(\cdot,t)||_{L^2(2B)}.$$

∎

The constant of the previous lemma can be chosen uniformly with respect to t in a closed interval $[t_1, t_2]$ for $t_1 > 0$:

COROLLARY 3.2. *Let $0 < t_1 < t_2$. There exists a constant $C_8 = C_8(R, t_1, t_2) > 0$ such that*

$$||u_0||_{L^1(\mathbb{R})} \leq C_8 ||u||_{L^2(2B \times (t_1,t_2))}.$$

What remains to be done is to get rid of the positiveness of u_0:

Proof of Theorem 1.3. Let $u^{\pm}$ be the solution to (1.1) with $u_0^{\pm} = \max\{\pm u_0, 0\}$ as initial condition respectively. Noticing that $u_0^{\pm} \geq 0$ and $u^{\pm} \geq 0$, Corollary 3.2 tells us that there exists a constant $C_8 > 0$ such that

$$||u_0^{\pm}||_{L^1(\mathbb{R}^n)} \leq C_8 ||u^{\pm}||_{L^2(2B\times(t_1,t_2))}.$$

Since $u = u^+ - u^-$, then

$$\begin{aligned} ||u_0||_{L^1(\mathbb{R}^n)} &= ||u_0^+||_{L^1(\mathbb{R}^n)} + ||u_0^-||_{L^1(\mathbb{R}^n)} \\ &\leq C_8 \left(||u||_{L^2(2B\times(t_1,t_2))} + ||u^-||_{L^2(2B\times(t_1,t_2))}\right). \end{aligned} \tag{3.5}$$

Let us analyze the two following operators:

$$\Lambda : u_0 \in L^1(B) \to u \in L^2(2B \times (t_1, t_2))$$

$$\Upsilon : u_0 \in L^1(B) \to u^- \in L^2(2B \times (t_1, t_2)),$$

and prove that Λ is a bounded and injective linear operator and Υ is a compact operator.

In effect, we use Young's inequality with $p = 1, q = 2$ and $r = 2$ (so that $\frac{1}{p} + \frac{1}{q} = \frac{1}{r} + 1$) to obtain

$$\begin{aligned} ||u^-(\cdot,t)||_{L^2(2B)} &\leq ||u_0^-||_{L^1(\mathbb{R}^n)} \frac{1}{(4\pi t)^{n/2}} ||e^{-|y|^2/4t}||_{L^2(\mathbb{R}^n)} \\ &\leq ||u_0^-||_{L^1(\mathbb{R}^n)} \frac{1}{(4\pi t)^{n/4}} \left(\int_{\mathbb{R}^n} \frac{1}{(4\pi t)^{n/2}} e^{-|y|^2/4t} dy\right)^{1/2} \\ &\leq ||u_0^-||_{L^1(\mathbb{R}^n)} \frac{1}{(4\pi t)^{n/4}}, \end{aligned}$$

where in the second step we used that $e^{-a/2t} \leq e^{-a/4t}$ for $a > 0$. From here we conclude that

$$||u^-||^2_{L^2(2B\times(t_1,t_2))} \leq ||u_0^-||^2_{L^1(\mathbb{R}^n)} \frac{1}{(4\pi)^{n/2}} \begin{cases} \log(t_2/t_1), & \text{if } n = 2 \\ \dfrac{1}{n/2-1}\left(\dfrac{t_1}{t_1^{n/2}} - \dfrac{t_2}{t_2^{n/2}}\right), & \text{if } n \neq 2. \end{cases}$$

Hence, there exists a constant $C > 0$ such that

$$||u^-||_{L^2(2B\times(t_1,t_2))} \leq C||u_0^-||_{L^1(\mathbb{R}^n)} \leq C||u_0||_{L^1(B)}, \tag{3.6}$$

and analogously, we have

$$||u^+||_{L^2(2B\times(t_1,t_2))} \leq C||u_0||_{L^1(B)}.$$

Since $u = u^+ - u^-$, Λ turns out to be a bounded operator:

$$||\Lambda u_0||_{L^2(2B\times(t_1,t_2))} = ||u||_{L^2(2B\times(t_1,t_2))} \leq C||u_0||_{L^1(B)}.$$

Let us verify the compactness of Υ. For this purpose we consider Υ as the composition of two operators $\Upsilon = \Upsilon_2 \circ \Upsilon_1$ where

$$\Upsilon_1 : u_0 \in L^1(B) \to u^- \in L^2(t_1, t_2; H^1(2B))$$

$$\Upsilon_2 : u^- \in L^2(t_1, t_2; H^1(2B)) \to u^- \in L^2(2B \times (t_1, t_2)).$$

We claim that Υ_1 is a bounded linear operator while Υ_2 is compact. In fact, thanks to (3.6) it suffices to estimate the derivatives in order to conclude the boundedness of Υ_1:

$$\nabla u^-(y,t) = \left(u_0^-(\cdot) * \nabla \frac{e^{-|\cdot|^2/4t}}{(4\pi t)^{n/2}} \right)(y) = \left(u_0^-(\cdot) * -\frac{\cdot}{2t} \frac{1}{(4\pi t)^{n/2}} e^{-|\cdot|^2/4t} \right)(y).$$

To estimate $||\nabla u^-(\cdot,t)||_{(L^2(2B))^n}$ we use Young's inequality with p, q and r as before getting

$$\begin{aligned} ||\nabla u^-(\cdot,t)||_{(L^2(2B))^n} &\leq ||u_0^-||_{L^1(\mathbb{R}^n)} \frac{1}{2(4\pi)^{n/2} t^{n/2+1}} ||y e^{-|y|^2/4t}||_{(L^2(\mathbb{R}^n))^n} \\ &= \frac{C}{t^{n/2+1}} ||u_0^-||_{L^1(\mathbb{R}^n)} \left(\int_{\mathbb{R}^n} |y|^2 e^{-|y|^2/2t} dy \right)^{1/2} \\ &= \frac{C}{t^{n/2+1}} ||u_0^-||_{L^1(\mathbb{R}^n)} \left(\int_0^\infty r^{n+1} e^{-r^2/2t} dr \right)^{1/2}, \end{aligned}$$

where we have used spherical coordinates. Notice that

$$\int_0^\infty r^{n+1} e^{-r^2/2t} dr = C(n) t^{n/2+1},$$

hence,

$$||\nabla u^-(\cdot,t)||_{(L^2(2B))^n} \leq C ||u_0^-||_{L^1(\mathbb{R}^n)} \frac{1}{t^{n/4+1/2}}.$$

Integrating in time from t_1 to t_2 we get

$$||\nabla u^-||^2_{L^2(2B \times (t_1,t_2))} \leq C ||u_0^-||^2_{L^1(\mathbb{R}^n)} \left(\frac{1}{t_1^{n/2}} - \frac{1}{t_2^{n/2}} \right).$$

Thus we have estimated the spatial derivative

$$||\nabla u^-||_{L^2(2B \times (t_1,t_2))} \leq C ||u_0^-||_{L^1(\mathbb{R}^n)} \leq C ||u_0||_{L^1(B)}.$$

In conclusion Υ_1 is bounded and thanks to Rellich-Kondrachov theorem Υ_2 is compact (see for instance theorem 6.3 in [1]). Consequently, Υ is a compact operator and from (3.5) and proposition 6.7 in [21] we conclude that Λ is a closed operator. Finally, strong unique continuation property of the heat equation implies the injectivity of Λ, thus, the open mapping theorem gives us the existence of a constant $C > 0$ such that

$$||u_0||_{L^1(\mathbb{R}^n)} \leq C ||\Lambda u_0||_{L^2(2B \times (t_1,t_2))} = C ||u||_{L^2(2B \times (t_1,t_2))}. \qquad \square$$

We finish this section by demonstrating Theorem 1.2:

Proof of Theorem 1.2. Let $t_1 = \tau + \varepsilon$ and $t_2 = T - \varepsilon$. From Theorem 1.3 there exists a constant $C_3 > 0$ such that

$$||u_0||_{L^1(\mathbb{R}^n)} \leq C_3 ||u||_{L^2(2B \times (\tau+\varepsilon, T-\varepsilon))} \leq C_3 ||u||_{L^2(\mathbb{R}^n \times (\tau+\varepsilon, T-\varepsilon))}.$$

From Theorem 2.1 we know that there exists a constant $C = C(\varepsilon)$ such that

$$||u||_{L^2(\mathbb{R}^n \times (\tau+\varepsilon, T-\varepsilon))} \leq C ||u||_{L^2(\omega \times (\tau,T))}$$

which concludes the proof. $\square$

Remark 3.3. The constant $C = C(\varepsilon)$ in the above inequality comes from Theorem 2.1 and is equal to (see Item I in the proof of Theorem 2.1)

$$C(\varepsilon) = \exp\left(\frac{\hat{s}K}{\varepsilon(T-\tau-\varepsilon)}\right)\frac{C}{\varepsilon(T-\tau-\varepsilon)}.$$

For instance, we can take $\varepsilon = (T-\tau)/4$ obtaining a constant for Theorem 1.2 of the form

$$C_2 = \exp\left(\frac{\hat{s}K}{(T-\tau)^2}\right)\frac{C_3}{(T-\tau)^2}.$$

4. Reconstruction of the initial conditions from measurements made on a curve. Another problem we are interested in is a stability result for the reconstruction of the compactly supported initial temperature u_0 for the heat equation (1.1) with $n = 1$, from observations made on a curve contained in $\mathbb{R} \times [0, \infty)$ and satisfying certain properties, a problem that arises naturally from the LSFM model that shall be explained in section section 5. In this section we shall prove Theorem 1.4.

The curve where observations are available is constructed as the graph of a positive function $\sigma : \mathbb{R} \to \mathbb{R}_+$ satisfying the $\sigma-$*properties* that we recall (see Figure 1 as a reference):

i) $\sigma \in C^1(\mathbb{R})$,
ii) $\sigma > 0$ for $y \in (a_1, a_2)$ and $\sigma(y) \equiv 0$ for $y \in (a_1, a_2)^c$, for some $a_1 < a_2$,
iii) there exists $\xi_1, \xi_2 > 0$ such that $\sigma' > 0$ in $(a_1, a_1 + \xi_1]$, $\sigma' < 0$ in $[a_2 - \xi_2, a_2)$ and $\sigma(a_1 + \xi_1) = \sigma(a_2 - \xi_2)$,
iv) $\dfrac{1}{\sigma'(y)} = \mathcal{O}\left(\exp\left(\dfrac{1}{\sigma(y)}\right)\right)$ as y goes to a_1^+, a_2^-.

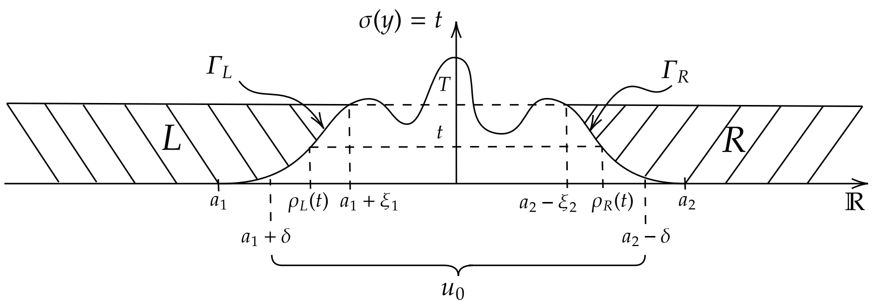

FIG. 1. *Representation of σ-properties and the relation of* $\operatorname{supp}(\sigma)$ *with the initial condition u_0 for Theorem 1.4.*

Defining $T := \sigma(a_1 + \xi_1)$ and as a consequence of conditions i)-iii), we can define the function $\rho_L(t) := \sigma^{-1}(t) \in C^1(0, T) \cap C[0, T]$, the inverse of σ to the right of a_1, by restricting σ to the interval $[a_1, a_1 + \xi_1]$. Thus, we can parameterize the curve Γ_L as $\{(\rho_L(t), t) : 0 \le t \le T\}$. Analogously, since σ is strictly decreasing in $[a_2 - \xi_2, a_2)$, we define $\rho_R(t) := \sigma^{-1}(t) \in C^1(0, T) \cap C[0, T]$ the inverse of σ to the left of a_2, then we parameterize Γ_R as $\{(\rho_R(t), t) : 0 \le t \le T\}$. The sketch of the proof is as follows: we define the set $\omega := [a_1, a_2]^c$ as the observation region and consider the time interval of observation as $(0, T)$. From Theorem 1.2, we are able to estimate u_0 with respect to the energy of u in $\omega \times (0, T)$. Certainly, the energy there is less than the energy up to the curves Γ_L and Γ_R, corresponding to the regions L and R in Figure 1. Consequently, to conclude Theorem 1.4 we need to estimate the energy in the region L with respect to the observations made on the curve Γ_L and do the same for the region R. This is exactly what Theorem 4.1 establishes:

THEOREM 4.1. *Let u be a solution of (1.1) with $n = 1$ and u_0 be the initial condition. Consider Γ_L the curve constructed from the function σ satisfying properties. If $u_0 \in L^1(\mathbb{R})$ with $\operatorname{supp}(u_0) \subset (a_1 + \delta, a_2 - \delta)$ then there exists a constant $C_9 = C_9(\sigma, \delta) > 0$ such that*

$$\frac{1}{2}\int_0^T \int_{-\infty}^{\rho_L(\tau)} |u(y,\tau)|^2 dy d\tau \leq C_9 T ||u_0||_{L^1(\mathbb{R})} ||u||_{L^1(\Gamma_L)}.$$

Proof. We define the left sided exterior energy as

$$I_L(t) := \frac{1}{2}\int_{-\infty}^{\rho_L(t)} |u(y,t)|^2 dy, \quad t \in [0,T),$$

and we differentiate it in order to get

$$\begin{aligned}
\frac{dI_L}{dt}(t) &= \frac{1}{2}u^2(\rho_L(t),t)\rho_L'(t) + \int_{-\infty}^{\rho_L(t)} u(y,t)u_t(y,t) \\
&= \frac{1}{2}u^2(\rho_L(t),t)\rho_L'(t) + \int_{-\infty}^{\rho_L(t)} u(y,t)u_{yy}(y,t) \\
&= \frac{1}{2}u^2(\rho_L(t),t)\rho_L'(t) + u(\rho_L(t),t)u_y(\rho_L(t),t) - \int_{-\infty}^{\rho_L(t)} |u_y(y,t)|^2 dy.
\end{aligned}$$

In what follows, we shall denote $g_L(t) := u(\rho_L(t),t)$ for $t \in (0,T)$, the measurements of u on Γ_L. Then

$$\begin{aligned}
\frac{dI_L}{dt}(t) &= \frac{1}{2}g_L^2(t)\rho_L'(t) + g_L(t)u_y(\rho_L(t),t) - \int_{-\infty}^{\rho_L(t)} |u_y(y,t)|^2 dy \\
&\leq \frac{1}{2}g_L^2(t)\rho_L'(t) + g_L(t)u_y(\rho_L(t),t).
\end{aligned} \tag{4.1}$$

We would like to bound the expression above so that the right-hand side depends only on the measurements g_L. Once we have that, we will integrate from 0 to t so that the left-hand side leads to $I_L(t)$ getting an estimate of I_L in terms of g_L.

For the first term in the right-hand side of (4.1) we see that Items i and ii imply that $\sigma'(y) \to 0$ when $y \to a_1$ and $\rho_L'(t) \to \infty$ when $t \to 0$, thus we need to control this latter growth with the decay of $g_L(t)$ in the same limit. For the second term we directly estimate $u_y(\rho_L(t),t)$.

I) Let us analyze the term $g_L(t)\rho_L'(t)$ in (4.1) for t in $(0,T)$, which turns out to be equivalent to study $\dfrac{g_L(\sigma(y))}{\sigma'(y)}$ for y in $(a_1, a_1 + \xi_1]$. Owing to the support of u_0 we have that

$$\left|\frac{g_L(\sigma(y))}{\sigma'(y)}\right| \leq \int_{a_1+\delta}^{a_2-\delta} \frac{|u_0(r)|}{(4\pi\sigma(y))^{1/2}\sigma'(y)} \exp\left(-\frac{|y-r|^2}{4\sigma(y)}\right) dr,$$

for $y \in (a_1, a_1 + \xi_1]$. The term multiplying $|u_0(r)|$ inside the previous integral may be uniformly bounded for $(y,r) \in [a_1, a_1 + \xi_1] \times [a_1 + \delta, a_2 - \delta]$. In effect, a singularity may occur when y approaches a_1, but if $|a_1 - y| < \delta/2$, and since $|a_1 - r| \geq \delta$, then we have

$$|a_1 - r| \leq |y-r| + |a_1 - y| < |y-r| + \delta/2 < |y-r| + |a_1 - r|/2,$$

and then

$$|y-r| > 1/2|a_1 - r| > \delta/2,$$

hence

$$\frac{1}{\sigma(y)^{1/2}\sigma'(y)}\exp\left(-\frac{|y-r|^2}{4\sigma(y)}\right) \leq \frac{1}{\sigma(y)^{1/2}\sigma'(y)}\exp\left(-\frac{\delta^2}{\sigma(y)}\right)$$

Plugging Item iv to the previous estimate we conclude the existence of a constant $C > 0$ such that

$$\left|\frac{g_L(y)}{\sigma'(y)}\right| \leq C\int_{a_1+\delta}^{a_2-\delta} |u_0(r)|dr = C||u_0||_{L^1(\mathbb{R})}.$$

II) Now we estimate $u_y(\rho_L(t), t)$ in $(0, T]$ for the second term in the right-hand side in (4.1), or, equivalently, $u_y(y, \sigma(y))$ in $(a_1, a_1 + \xi_1]$. First recall that

$$u_y(y, \sigma(y)) = \int_{a_1+\delta}^{a_2-\delta} \frac{u_0(r)}{\sqrt{4\pi\sigma(y)}}\exp\left(-\frac{(y-r)^2}{4\sigma(y)}\right)\frac{-|y-r|}{2\sigma(y)}dr.$$

Again, the term accompanying $|u_0(r)|$ is uniformly bounded for $(y, r) \in [a_1, a_1 + \xi_1] \times [a_1 + \delta, a_2 - \delta]$ by continuity. In conclusion,

$$|u_y(\rho_L(t), t)| \leq C\int_{a_1+\delta}^{a_2-\delta} |u_0(r)|dr = C||u_0||_{L^1(\mathbb{R})}.$$

Bringing all the previous estimates together along with (4.1) it yields

$$\begin{aligned}\frac{dI_L}{dt} &\leq \frac{1}{2}|g_L^2(t)||\rho_L'(t)| + |g_L(t)||u_y(\rho_L(t), t)| \\ &\leq C||u_0||_{L^1(\mathbb{R})}|g_L(t)|,\end{aligned}$$

thus, integrating from 0 to τ leads to

$$I_L(\tau) \leq C||u_0||_{L^1(\mathbb{R})}\int_0^\tau |g_L(t)|dt.$$

Integrating again in time from 0 to T, we get that

$$\begin{aligned}\frac{1}{2}\int_0^T\int_{-\infty}^{\rho_L(\tau)} |u(y,\tau)|^2 dy d\tau &= \int_0^T I_L(\tau)d\tau \\ \text{(Fubini)} \quad &\leq CT||u_0||_{L^1(\mathbb{R})}\int_0^T |g_L(t)|dt \\ &= CT||u_0||_{L^1(\mathbb{R})}||u||_{L^1(\Gamma)}.\end{aligned}$$ □

Remark 4.2. So far, we have estimated the energy in region L (see Figure 1) with respect to the measurements available on Γ_L. Analogously, we can do the same to estimate the energy contained in region R with respect to measurements available on Γ_R. Same calculations as before leads to

$$\frac{1}{2}\int_0^T\int_{\rho_R(\tau)}^{\infty} |u(y,\tau)|^2 dy d\tau \leq C_9 T||u_0||_{L^1(\mathbb{R})}||u||_{L^1(\Gamma_R)}.$$

We are now able to conclude the desired stability:

Proof of Theorem 1.4. Let $\omega = [a_1, a_2]^c$. By Theorem 1.2 there exists a constant $C_2 > 0$ such that

$$||u_0||_{L^1(\mathbb{R})} \leq C_2 ||u||_{L^2(\omega\times(0,T))}. \tag{4.2}$$

Moreover, Theorem 4.1 implies

$$\begin{aligned} ||u||^2_{L^2(\omega\times(0,T))} &\leq \int_0^T \int_{-\infty}^{\rho_L(\tau)} |u(y,\tau)|^2 dy d\tau + \int_0^T \int_{\rho_R(\tau)}^{\infty} |u(y,\tau)|^2 dy d\tau \\ &\leq C_9 ||u_0||_{L^1(\mathbb{R})} T(||u||_{L^1(\Gamma_L)} + ||u||_{L^1(\Gamma_R)}). \end{aligned} \tag{4.3}$$

We conclude with (4.2) and (4.3). ∎

Remark 4.3. The stability constant decreases with respect to T, which is natural from the fact that a larger T means we use more information contained in our measurements. In fact, taking $\varepsilon = T/4$ (as in Remark 3.3) the constant turns out to be

$$C_9 C_2^2 T = C_9 \exp\left(\frac{\hat{s}K}{T^2}\right)\frac{C_3^2}{T^4} T = C_9 \exp\left(\frac{\hat{s}K}{T^2}\right)\frac{C_3^2}{T^3}.$$

5. Stability for 2D LSFM inverse problem. LSFM is an instrument that allows researchers to observe live specimens and dynamical processes by attaching fluorophores to certain cellular structures. After attaching fluorophores, the process of imaging the specimen is carried out in two steps: illumination (or excitation) and fluorescence. In the first stage a slice of the object is illuminated with a light sheet, exciting fluorophores therein. Subsequently, in the second stage, a camera measures the fluorescent radiation obtaining a two dimensional image. The microscope then scans plane by plane so that a stack of two dimensional images is collected, which represents the three dimensional object. In [6] a two dimensional model is considered, hence, the illumination takes the form of a laser beam issued from different heights instead of light sheets. The Fermi-Eyges pencil-beam equation governs the illumination process, describing the space and angular distribution of photons. During the fluorescence step, photons coming out from fluorescent molecules propagate in several directions reaching the camera. The Radiative Transport Equation is used to model this second step [2]. The whole process is represented in Figure 2.

Let us recall some of the definitions given in [6] for the setting of the LSFM model: we consider the domain $\Omega \subseteq [0, s_1] \times [-y_1, y_1]$ as the object to be observed. For $y \in [-y_1, y_1]$ we define $x_y = \inf\{x : (x, y) \in \Omega\}$. For $s \in [0, s_1]$ we define

$$Y_s = \{y \in [-y_1, y_1] : x_y \leq s\}, \quad s^- = \inf\{s : Y_s \neq \emptyset\}$$

Let s^+ be the largest s such that $[x_y, s] \times \{y\} \subseteq \Omega$. For a fixed $s \in [s^-, s^+]$ we define $\underline{y} = \underline{y}(s) = \inf(Y_s)$ and $\bar{y} = \bar{y}(s) = \sup(Y_s)$, which, in what follows, we shall call them *object top boundary* and *object bottom boundary* respectively. For s^+ we denote $y^+ = \bar{y}(s^+)$ and $y^- = \underline{y}(s^+)$. Finally, we define the function $\gamma : Y_s \to [0, s^+]$ as $\gamma(y) = x_y$. See Figure 3 for these definitions.

There are two physical parameters involved during the illumination stage: the attenuation λ, corresponding to a measure of absorption of photons, and ψ corresponding to a measure of scattering which explains the broadening of the laser beam shown in Figures 2 and 3. On the other hand, in the second stage the third physical parameter involved is the attenuation a, a measure of absorption of fluorescent radiation. We assume that $\lambda, a \in C_{pw}(\overline{\Omega})$, $\psi \in C^1(\overline{\Omega})$, and $\gamma \in C^1(Y_s)$. According to

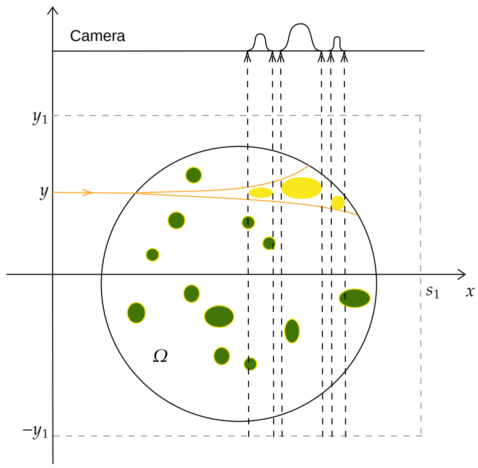

FIG. 2. *Representation of illumination and fluorescence stages in LSFM. A laser beam is emitted at height y and illuminates the object from left. Due to scattering, photons are deflected from their original direction. Some fluorophores got excited (in yellow), the others (in dark green) will not fluoresce. Since we assume the camera is collimated, it will measure only photons emitted in straight vertical direction.*

[6], the measurement obtained by the camera at pixel s when illumination is made at height $y \in Y_s$ is given by the next expression:

(5.1)
$$p(s,y) = c \cdot \exp\left(-\int_{\gamma(y)}^{s} \lambda(\tau,y)d\tau\right) \int_{\mathbb{R}} \frac{\mu(s,r)e^{-\int_r^\infty a(s,\tau)d\tau}}{\sqrt{4\pi\sigma(s,y)}} \exp\left(-\frac{(r-h)^2}{4\sigma(s,y)}\right) dr,$$

where

$$\sigma(s,y) = \frac{1}{2}\int_{\gamma(y)}^{s} (s-\tau)^2 \psi(\tau,y)d\tau. \tag{5.2}$$

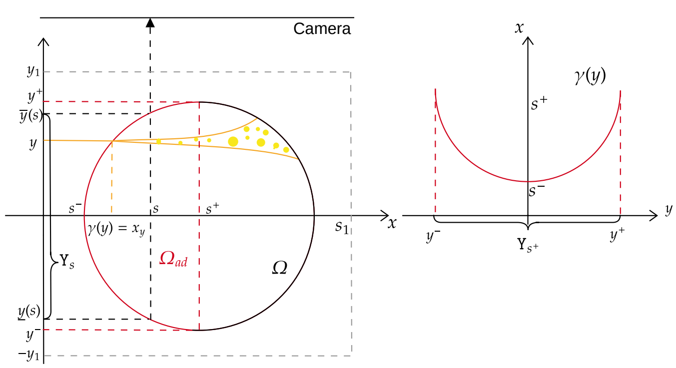

FIG. 3. *Left figure presents the definition of the quantities s^- and s^+ and the set Y_{s^+} for a generic set Ω. Right figure shows the function γ and its domain Y_{s^+} in the new coordinates.*

In what follows, we shall fix s and consider the functions $p(y) := p(s, y)$ and $\sigma(y) := \sigma(s, y)$, so that p represents the measurements obtained at a pixel s, as a function of the height of illumination y. Besides, we identify p and σ with their zero-extension to the whole real line. If we consider u as the solution of equation (1.1) with $n = 1$ and initial condition $u_0(y) = \mu(s, y)e^{-\int_y^\infty a(s,\tau)d\tau}$ then we have the following relation:

$$u(y, \sigma(y)) = \frac{1}{c}\exp\left(\int_{\gamma(y)}^{s} \lambda(\tau, y)d\tau\right)p(y), \quad \forall y \in \mathbb{R}. \tag{5.3}$$

The above equation tells us that we have measurements of the solution of the heat equation in $\mathbb{R}$ on the curve $\Gamma := \{(y, \sigma(y)) : y \in \mathbb{R}\} \subseteq \mathbb{R} \times [0, \infty)$. Then, if we want a stability result for this inverse problem, it only remains to verify the hypothesis of Theorem 1.4. For this purpose, let us define a set of admissible sources: let $\widetilde{\Omega} \subsetneq \Omega$ be an open subdomain strictly contained in Ω and define $\mathcal{B}$ the set of admissible sources as (see Figure 4):

$$\mathcal{B} := \{\mu \in L^1(\mathbb{R}^2) : \mu(s, \cdot) \in L^1(\mathbb{R}), \forall s \in (s^-, s^+), \operatorname{supp}(\mu) \subset \widetilde{\Omega}.\} \tag{5.4}$$

The main result of this section is the following theorem

Theorem 5.1. *Let $\mu \in \mathcal{B}$, $s \in (s^-, s^+)$. Then, there exists a constant $C_{10} = C_{10}(\sigma, s) > 0$ such that*

$$\left|\left|\mu(s,\cdot)e^{-\int_\cdot^\infty a(s,\tau)d\tau}\right|\right|_{L^1(\mathbb{R})} \leq C_{10}\left(\left|\left|\frac{1}{c}p(\cdot)e^{\int_{\gamma(\cdot)}^{s}\lambda(\tau,\cdot)d\tau}\right|\right|_{L^1((\underline{y},\underline{y}+\xi_1)\cup(\bar{y}-\xi_2,\bar{y}))}\right),$$

and therefore

$$||\mu(s,\cdot)||_{L^1(\mathbb{R})} \leq C_{11}||p||_{L^1((\underline{y},\underline{y}+\xi_1)\cup(\bar{y}-\xi_2,\bar{y}))},$$

where

$$C_{11} = \frac{C_{10}}{c}\exp(||a(s,\cdot)||_{L^1(\mathbb{R})} + ||\lambda||_{L^\infty(\mathbb{R}^2)}(s - s^-)).$$

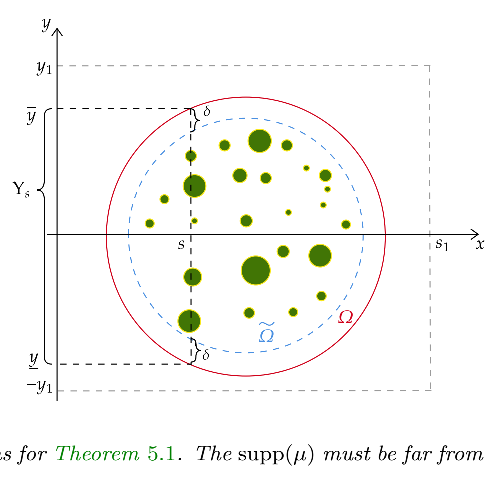

Fig. 4. *Assumptions for Theorem 5.1. The* $\operatorname{supp}(\mu)$ *must be far from* $\partial\Omega$*, which is accomplished by letting* $\mu \in \mathcal{B}$.

Proof. Recall that we consider $\mu(s,\cdot)e^{-\int_\cdot^\infty a(s,\tau)d\tau}$ as the initial condition of the heat equation in $\mathbb{R}$ and measurements are given according to (5.3). As in Figure 4, since $\mu \in \mathcal{B}$, for the fixed s there exists a constant $\delta = \delta(s) > 0$ such that $\mu(s,\cdot) \equiv 0$ in $(\underline{y}, \underline{y}+\delta) \cup (\bar{y}-\delta, \bar{y})$, *i.e.*, $\mathrm{supp}(\mu(s,\cdot)e^{-\int_\cdot^\infty a(s,\tau)d\tau}) \subset (\underline{y}+\delta, \bar{y}-\delta)$. Now, it suffices to prove that σ satisfies the $\sigma-$properties:

i) From (5.2) we have that

$$\sigma'(y) = -\frac{1}{2}\gamma'(y)(s-\gamma(y))^2\psi(\gamma(y),y) + \frac{1}{2}\int_{\gamma(y)}^s (s-\tau)^2 \frac{\partial \psi}{\partial y}(\tau,y)d\tau, \quad \text{for } y \in Y_s. \tag{5.5}$$

By the regularity of γ and ψ, we get that $\sigma \in C^1(Y_s)$. Furthermore $\sigma'(\underline{y}) = \sigma'(\bar{y}) = 0$ since $\gamma(\bar{y}) = \gamma(\underline{y}) = s$. We conclude that $\sigma \in C^1(\mathbb{R})$ by noticing that $\sigma'(y) = 0$ for $y \notin Y_s$.

ii) From (5.2) and the zero-extension of σ, it is direct that $\sigma > 0$ for $y \in (\underline{y}, \bar{y})$ and $\sigma(y) = 0$ for $y \in (\underline{y}, \bar{y})^c$.

iii) From (5.5) we get that

$$\sigma'(y) \geq \frac{1}{2}(s-\gamma(y))^2\left[-\gamma'(y)\psi(\gamma(y),y) - \int_{\gamma(y)}^s |\psi_y(\tau,y)|d\tau\right]. \tag{5.6}$$

Let $m := \inf_{(x,y)\in\overline{\Omega}} |\psi(x,y)|$ and $M := \sup_{(x,y)\in\overline{\Omega}} \left|\frac{\partial\psi}{\partial y}(x,y)\right|$. Then

$$\frac{2\sigma'(y)}{(s-\gamma(y))^2} \geq -\gamma'(y)m - \frac{1}{3}(s-\gamma(y))M \xrightarrow[y\to\underline{y}^+]{} -\gamma'(\underline{y})m$$

Recalling that $\gamma'(\underline{y}) < 0$ we conclude the existence of $\xi_1 > 0$ such that $\sigma' > 0$ in $(\underline{y}, \underline{y}+\xi_1]$. By letting $y \to \bar{y}^-$ instead of $\underline{y}^+$ we obtain the existence of $\xi_2 > 0$ such that $\sigma' < 0$ in $[\bar{y}-\xi_2, \bar{y})$. Furthermore, we redefine ξ_1 and ξ_2 such that $\sigma(\underline{y}+\xi_1) = \sigma(\bar{y}-\xi_2) = \min\{\sigma(\underline{y}+\xi_1), \sigma(\bar{y}-\xi_2)\}$.

iv) Finally, we not only prove that $\frac{1}{\sigma'(y)} = \mathcal{O}\left(\exp\left(\frac{1}{\sigma(y)}\right)\right)$ as y goes to $\underline{y}^+$ and $\bar{y}^-$ but $\lim_{y\to\underline{y}^+} \frac{1}{\sigma'(y)}\exp\left(-\frac{1}{\sigma(y)}\right) = 0$. For the limit as y goes to $\bar{y}^-$ the argument is analogous. In effect, from (5.6) we get that

$$\sigma'(y) \geq C(s-\gamma(y))^2, \quad \text{for } y \in (\underline{y}, \underline{y}+\xi_1].$$

Secondly, notice that

$$\sigma(y) = \frac{1}{2}\int_{\gamma(y)}^s (s-\tau)^2\psi(\tau,y)d\tau \leq C(s-\gamma(y))^3.$$

Then, since $\gamma(\underline{y}) = s$ we have that

$$\begin{aligned} \frac{1}{\sigma'(y)}\exp\left(-\frac{1}{\sigma(y)}\right) &\leq \frac{1}{C(s-\gamma(y))^2}\exp\left(-\frac{1}{C(s-\gamma(y))^3}\right) \\ &\to 0, \quad \text{as } y \to \underline{y}^+, \end{aligned}$$

We conclude by applying Theorem 1.4. ∎

Remark 5.2. Certainly, the stability constant C_{10} is equal to C_4 in Theorem 1.4. If we define $T_1 := \sigma(a_1 + \xi_1)$ and $T_2 := \sigma(a_2 + \xi_2)$, then we may consider the time $T = \min\{T_1, T_2\}$ as in Figure 5. In the next section, we shall study the dependence of the stability constant with respect to this variable T.

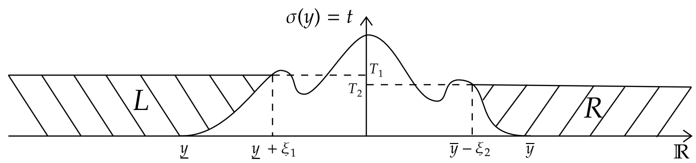

FIG. 5. *Curve Γ on which measurements are available for LSFM model. In this example, we must consider the variable $T = T_2$.*

6. Numerical results in LSFM.

In this section, we analyze the behavior of the stability constant C_{10} given by Theorem 5.1. Mainly, we observe its dependency with respect to the variable T, defined by $T = \min\{T_1, T_2\}$, as commented in Remarks 4.3 and 5.2 (see Figure 5). We recall that the definition of T depends on the monotonicity of function σ defined in terms of the diffusion coefficient ψ in (5.2). Moreover, since the result given by Theorem 5.1 considers $\mu \in \mathcal{B}$, *i.e.* $\text{supp}(\mu) \subset \widetilde{\Omega}$, we show below that the constant C_{10} increases as the support of μ gets closer to the boundary of $\widetilde{\Omega}$, and the stability is not guarantied when we reach $\partial\widetilde{\Omega}$. We devote part of the experiments to analyze the observation interval $(\underline{y}, \underline{y} + \xi_1) \cup (\bar{y} - \xi_2, \bar{y})$, to understand not only the stability of reconstructing $\mu(s, \cdot)$ but also, the quality of its reconstruction.

6.1. Datasets.

We consider three datasets as shown in Figure 6. Source in `Dataset 1` describes a random distributed fluorescent sources supported in a circular domain. The attenuation λ in the illumination stage is constant and supported in Ω with radius greater than the support of μ to guarantee the hypothesis (5.4). This latter condition is also considered in the other two datasets. The source in `Dataset 2` is also randomly distributed in a support with a particular shape, this choice has the purpose of analyzing the behavior of the function σ in terms of its increasing and decreasing intervals as we will see in subsection 6.3 below. The attenuation is also constant as before. The third dataset aims to be closer to a real LSFM applications. We have simulated a *zebrafish larvae* merged in an circular support with a constant attenuated substance. The source in real experiments determines, for example, zones with multicellular chemical reactions. The attenuation is composed by a constant background and a contribution given by the presence of the fluorescent source, *i.e*, $\lambda = w_1 \mathbb{1}_{\widetilde{\Omega}} + w_2\mu$. In all cases, the diffusion term is defined by $\psi = c\lambda$, with $c > 0$, which means that the diffusion is proportional to the attenuation properties of the medium.

Our first interest is to show that the constant C_{10} in Theorem 5.1 has a relationship with the support of μ, *i.e.* the further we are from the boundary of $\tilde{\Omega}$, the better the stability of reconstructing μ is. This analysis is based on the condition number of a matrix A_s that we detail below in subsection 6.2. We use `Dataset 1` and `Dataset 2` to observe the proposed assay.

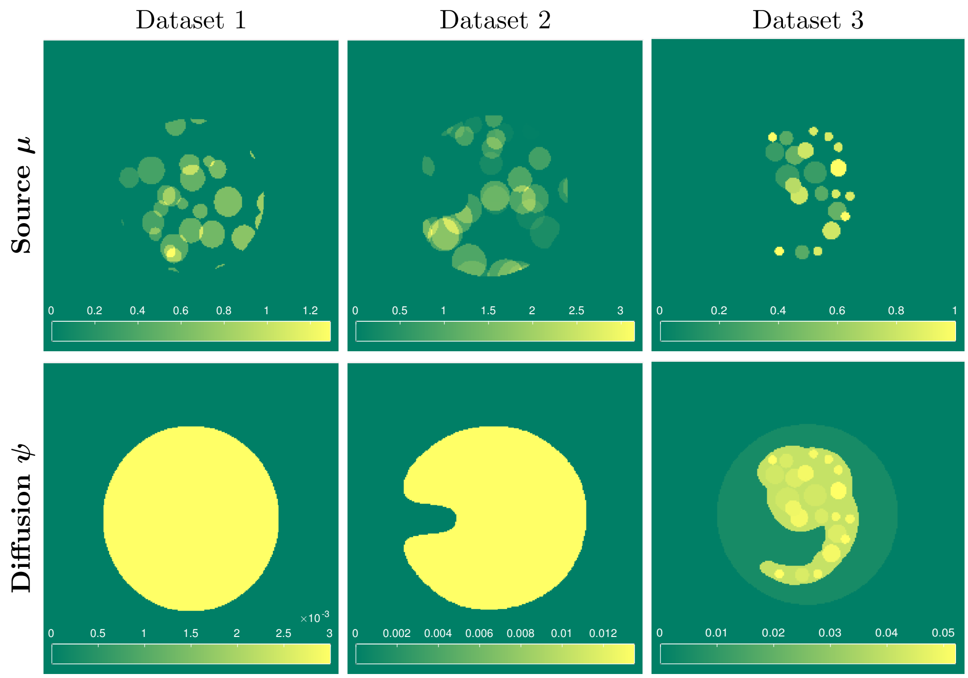

FIG. 6. *Data sets. In the upper row, the sources μ for three different supports and in the bottom row, the corresponding diffusion maps.* `Dataset 1` *considers random distributed circles with constant attenuation.* `Dataset 2` *is defined on an irregular support useful to analyse the function σ.* `Dataset 3` *aims to be closer to a real experiment where a zebrafish embryo profile is simulated.*

6.2. Condition number of matrix $\boldsymbol{A_s}$ in terms of supp $\boldsymbol{\mu(s,\cdot)}$. In the discrete case, as it was detailed in [6], recovering μ is established as the solution of a linear system

$$\boldsymbol{A}\boldsymbol{\mu} = \boldsymbol{b}$$

where $\boldsymbol{A} \in \mathbb{R}^{m\times n}$ links the vectorized source $\boldsymbol{\mu} \in \mathbb{R}^n$ to the array of measurements $\boldsymbol{b} \in \mathbb{R}^m$. This is a direct consequence of the linear nature of measurements $p(s, y)$ in (5.1) respect to the unknown variable μ.

The set of measurements considers m_1 heights of excitation (illuminations) and m_2 detectors using just one camera. The excitation process is made from right and left sides and, consequently, the number of observations is $m = 2 \cdot m_1 \cdot m_2$.

As we are interested on $\mu(s, \cdot)$ for a given $s \in (s^-, s^+)$ based on Theorem 5.1, we use the condition number of a submatrix $\boldsymbol{A}_s$ of $\boldsymbol{A}$ to know how stable is to reconstruct the restriction of $\boldsymbol{\mu}$ to the depth s. This matrix $\boldsymbol{A}_s$ chooses the rows of $\boldsymbol{A}$ associated to the observations receipted by the detector s, one for each illumination, *i.e.* $\boldsymbol{A}_s$ has $m_s = 2 \cdot m_1$ rows. Furthermore, we want to study the stability in terms of supp μ, so we choose the columns of $\boldsymbol{A}$ where the support of $\mu(s, \cdot)$ is defined, this means that we focus on the pixels where the discrete source is nonzero. Observe that for larger values of the radius, more columns of $\boldsymbol{A}$ are taken. With this row and column sampling, we determine the submatrix $\boldsymbol{A}_s$ whose condition number value (cond(A_s)) is represented in Figure 7 for `Dataset 1` and `Dataset 2` in upper and bottom rows, respectively.

For `Dataset 1`, the circular shape of supp μ allows us to easily control its proximity to $\widetilde{\Omega}$. As it is presented in the right hand side of Figure 7, we test radius from 0.55 until 0.8 in $\Omega = [0,2] \times [-1,1]$, the maximum value $r = 0.8$ is the radius that defines $\widetilde{\Omega}$. As it is expected, the condition number increases when the support of μ tends to the boundary of $\widetilde{\Omega}$, this is shown in the left hand side of Figure 7. We also include different values of s to observe that this condition number also depends on this variable at least when the diffusion term ψ is constant. The values of s varies from 0.66 to 0.96, and the value of $\mathrm{cond}(A_s)$ tends to increase when we go deeper in the object. This makes sense in the light of LSFM applications since the middle part of the object is harder to be observed directly from the measure process, and solving the inverse problem is also challenging in this zone. A similar result is observed for `Dataset 2`, we have define five different sizes of supports and five depths s. The condition number of the corresponding matrices A_s increases when we get closer to the boundary of $\widetilde{\Omega}$. We also observe that the conditioning is worse for small values of s compare to the previous example, this is also related to the number of illuminations in each depth s, we will observe this in detail in subsection 6.4.

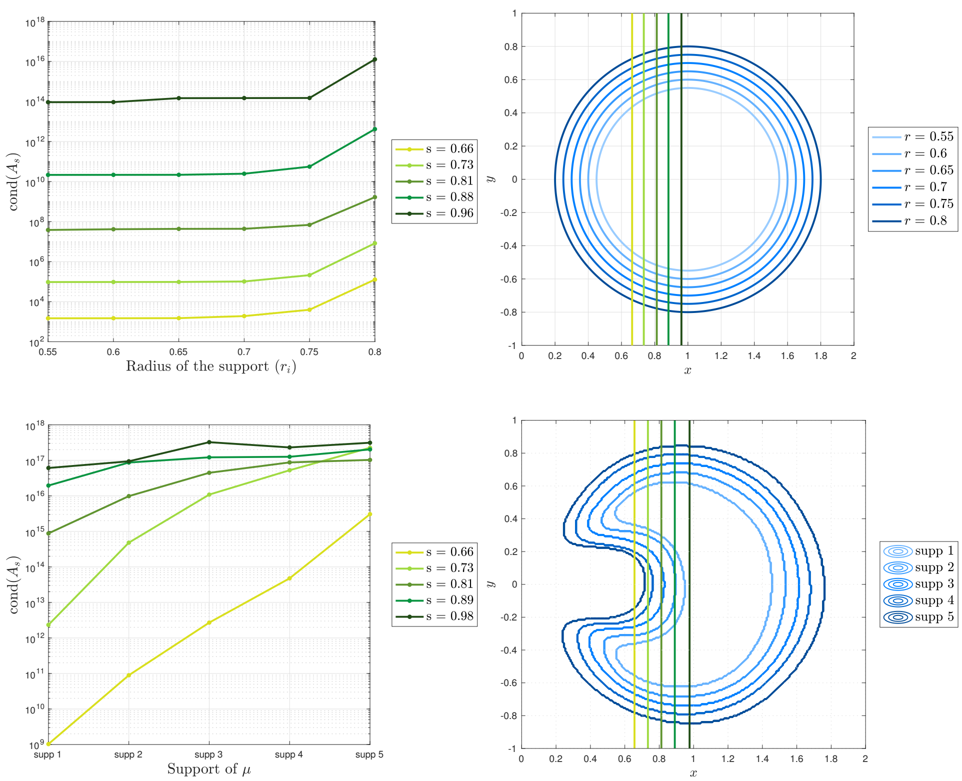

FIG. 7. Left: *Condition number of matrix A_s in terms of the size of the support of μ for* `Dataset 1` *in the upper row and, for* `Dataset 2` *in the bottom row. Each line is related to the depth s as is shown in right figure.* Right: *The different supports in terms of support and depths s considered to computed the conditional number.*

In the subsection below, we study in detail the observation intervals $(\underline{y}, \underline{y} + \xi_1) \cup (\bar{y} - \xi_2, \bar{y})$ for a particular choice of s using the three datasets. This will be used later to compare the condition number of A_s when the illuminations are taken in the aforementioned interval or in the complete interval $(\underline{y}, \bar{y})$.

6.3. Object top and bottom boundaries. Here, we use our three sets of data to identify the σ-properties in each case. We aim to do a representation as the one shown in Figure 5.

For `Dataset 1`, the shape of Γ is a symmetric curve respect to the origin as is shown in Figure 8. This is a direct consequence of the constant diffusion ψ and a circular domain $\widetilde{\Omega}$ centered in the origin. We observe that $\sigma'(y) > 0$ in the interval $(-0.789, 0)$ and $\sigma'(y) < 0$ in $(0, 0.789)$, so $T_1 = T_2 = 3.109 \times 10^{-4}$ and is reached at $y = 0$. According with these values, the observation set $(\underline{y}, \underline{y} + \xi_1) \cup (\bar{y} - \xi_2, \bar{y})$ specified in Theorem 5.1 corresponds to the interval $(-0.789, 0.789)$.

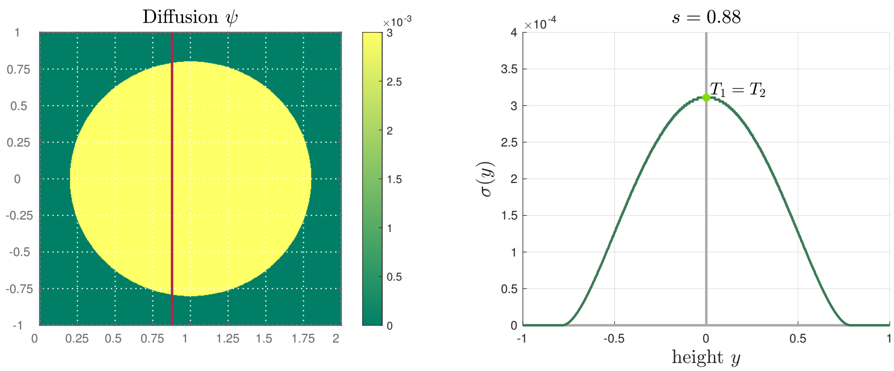

FIG. 8. *Curve Γ for* `Dataset 1` *at $s = 0.88$. On the left, the constant diffusion defined over a circle with centre in the origin and $r = 0.8$. The vertical line defines the observed value of s. On the right, $\sigma(y)$ defines a symmetric curve Γ where $T = T_1 = T_2$.*

For `Dataset 2`, the curve Γ presents a convexity near the origin as is shown in Figure 9. This behaviour is due to the particular shape of $\widetilde{\Omega}$, the diffusion map presents a lateral sag that is not perfectly symmetric respect to the origin in y-axis, as a consequence, the values of $T_1 = \sigma(\underline{y} + \xi_1)$ and $T_2 = \sigma(\bar{y} - \xi_2)$ are slightly different. More precisely, $T_1 = 8.48 \times 10^{-4}$, $T_2 = 8.31 \times 10^{-4}$ and $T = T_2$. In this case, $\sigma'(y) > 0$ in $(\underline{y}, \underline{y} + \xi_1) = (-0.589, -0.232)$ and $\sigma'(y) < 0$ in $(\bar{y} - \xi_2, \bar{y}) = (0.174, 0.577)$.

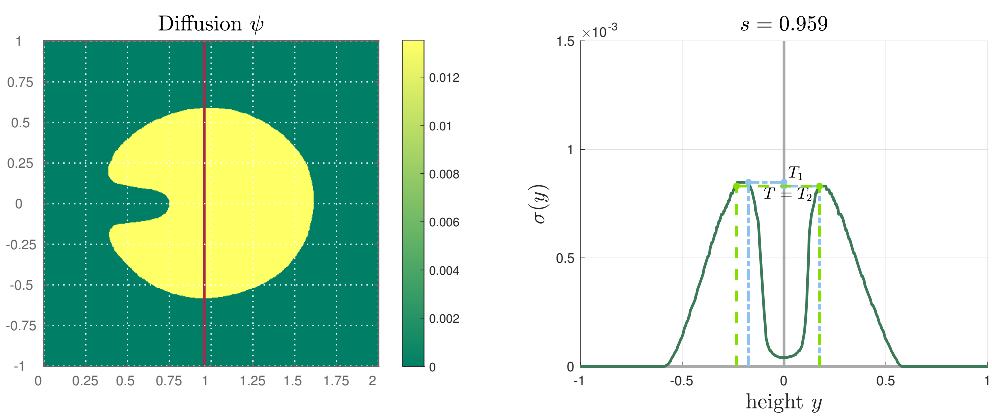

FIG. 9. *Curve Γ for* `Dataset 2` *at $s = 0.959$. On the right, the constant diffusion where the vertical line defines the observed value of s. On the left, $\sigma(y)$ defines the curve Γ with a convexity around the origin. T_1 and T_2 are marked as dots and, increasing and decreasing zones are identified.*

For `Dataset 3`, the curve Γ has a different behaviour due to the particular election of the diffusion term. As before, we have identified the illumination intervals based on the values of T_1 and T_2 as is presented in Figure 10. In this case, $T = T_2$ and $\underline{y} + \xi_1 = -0.362$ and $\bar{y} - \xi_2 = 0.311$. As the support of σ is $[\underline{y}, \overline{y}] = [-0.601, 0.553]$, the illumination set in this case is defined over $(-0.601, -0.362) \cup (0.311, 0.553)$.

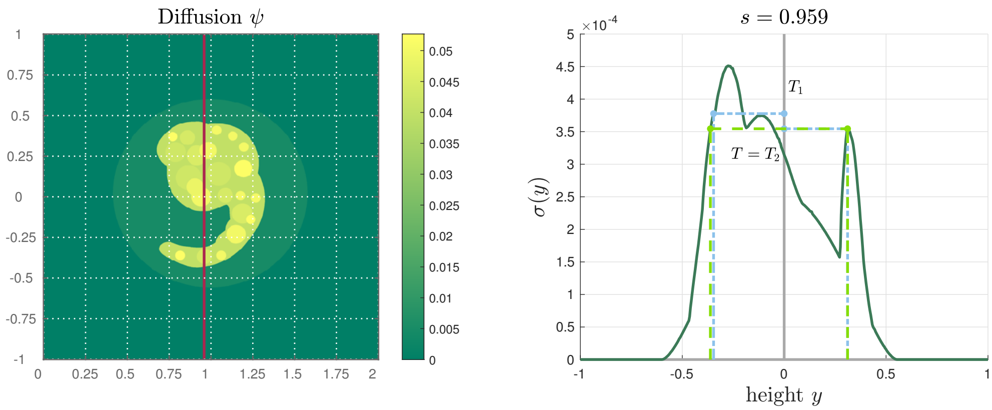

FIG. 10. *Curve Γ for `Dataset 3` at $s = 0.959$. On the right, the diffusion caused by the presence of the specimen, the fluorescent source and the circular medium where the zebrafish is merged. The vertical line defines the observed value of s. On the left, $\sigma(y)$ defines the curve Γ and, the values of T_1 and T_2 are marked as dots.*

Once we have determined the observations regions, we use this (limited-) information below to reconstruct $\mu(s, \cdot)$ and compare it with the reconstruction obtained when a full set of observations is used. This last experiment aims to show the assertion made in Remark 4.3. Let us first observe the conditioning of a matrix $\boldsymbol{A}_s$ when full illumination are considered compared to the limited set of illuminations defined by σ-properties. For this experiment, we have considered `Dataset 2` and `Dataset 3` where full and limited illuminations differ. In Figure 11, we present function σ for different values of s, as in Figures 9 and 10, we determine the observation intervals that are also detailed in Table 1. Once, we select the illumination set, we can choose the corresponding rows of the matrix $\boldsymbol{A}$ to build $\boldsymbol{A}_s$ in each case. The condition number of $\boldsymbol{A}_s$ is plotted in the right hand side of Figure 11 for `Dataset 2` in the top row and, for `Dataset 3` in the bottom row. The main difference between the dotted and continued lines is what we expected by Theorem 5.1, the stability of reconstructing $\mu(s, \cdot)$, observed through the condition number of $\boldsymbol{A}_s$, is worse when we have less observations, *i.e.* when the value of T is smaller as in Remark 4.3. For `Dataset 3` in the full-observation case, the condition number does not have strict growth as we increase the variable s, this is due to the variability of the diffusion map.

Finally, we illustrate the measurement process using `Dataset 3`, we explain how to get the set of measurements after illuminating and counting photons in one camera. We select the data associated to a particular s to reconstruct $\mu(s, \cdot)$ when limited and full illuminations are considered.

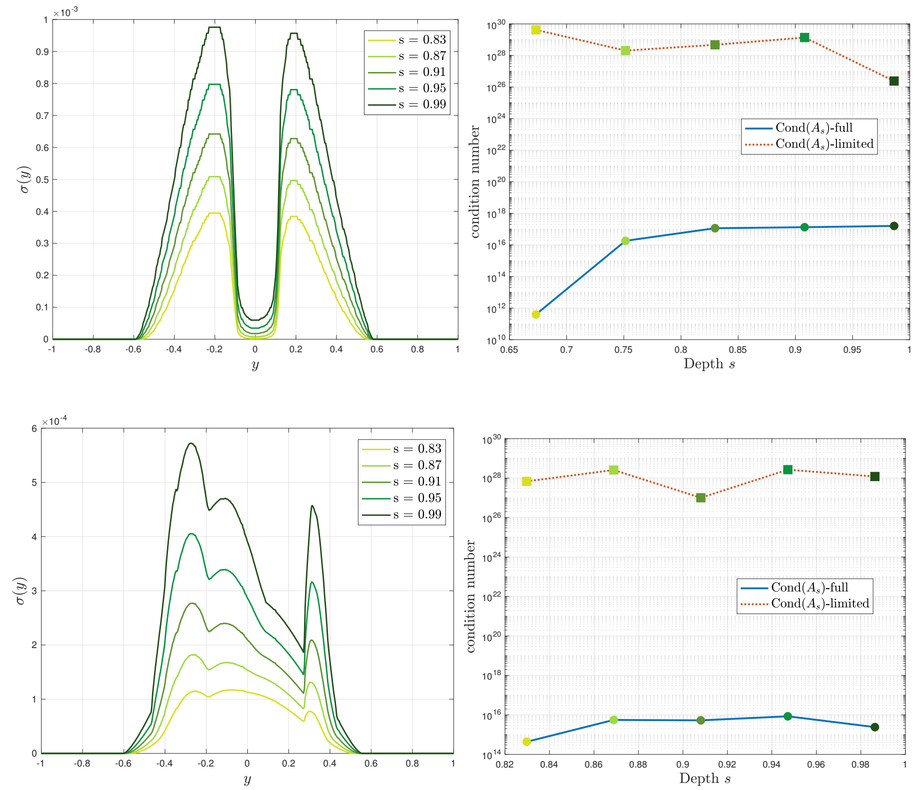

FIG. 11. *Condition number of $\boldsymbol{A}_s$ matrix. Top row: results for* `Dataset 2` *when different values of s are considered. On the left hand, the σ function is plotted to identify the observation intervals determined by the top and bottom boundaries. On the right hand, cond(A_s) for full and limited illuminations are plotted. The bottom row considers the same results for* `Dataset 3`*. The limited case depends on the intervals defined in Table 1.*

TABLE 1
Observation intervals for `Dataset 2` *and* `Dataset 3`*. For different values of s between 0.67 and 0.99, we analyze the behaviour of σ given in Figure 11 to determine the intervals $(\underline{y}, \underline{y}+\xi_1) \cup (\bar{y}-\xi_2, \bar{y})$ as in Figures 9 and 10.*

s	`Dataset 2`	`Dataset 3`
0.67	$(-0.566, -0.233) \cup (0.174, 0.562)$	$(-0.577, -0.354) \cup (0.295, 0.534)$
0.75	$(-0.577, -0.233) \cup (0.174, 0.569)$	$(-0.597, -0.358) \cup (0.303, 0.55)$
0.83	$(-0.585, -0.233) \cup (0.174, 0.573)$	$(-0.597, -0.358) \cup (0.307, 0.55)$
0.91	$(-0.589, -0.233) \cup (0.174, 0.577)$	$(-0.601, -0.362) \cup (0.311, 0.554)$
0.99	$(-0.589, -0.233) \cup (0.174, 0.577)$	$(-0.605, -0.366) \cup (0.311, 0.558)$

6.4. Reconstructions based on parameter $\boldsymbol{T}$. In this part, we aim to reconstruct $\mu(s,\cdot)$ for a fixed value of s using `Dataset 3`. We will see that this reconstruction is stable in terms of Theorem 5.1. The resulting set of measurements after illuminating along all possible heights is represented in Figure 12. We can observe a blurred image which represents the effects of the diffusion (scattering) during the excitation stage. These measurements were also perturbed by Poisson noise to avoid inverse crime during the reconstruction.

In Figure 13, we present the reconstruction of $\mu(s, y)$ for $s = 0.969$, the left hand

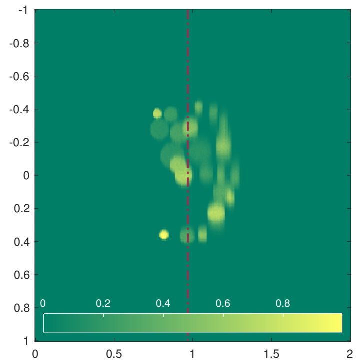

FIG. 12. *Noise measurements for* `Dataset 3`. *For each illumination height y in y-axis, the corresponding row in the image represents the number of photons (scaled as intensity) that is observed by the camera after the excitation beam is emitted at the point $(0, y)$. The vertical line marks the depth s considered to reconstruct $\mu(s,\cdot)$.*

side of this figure presents the σ function needed to determine the object top and bottom boundaries. As was analyzed before, the illuminations used in Theorem 5.1 that determine measurements are taken in the set $I = (-0.602, -0.375) \cup (0.344, 0.555)$. On the right side of Figure 13, we show the source $\mu(s, y)$ as ground truth, the reconstruction using only illuminations over I (limited illuminations) and, the reconstruction for illuminations over $(-0.602, 0.555)$ (full illuminations). These reconstructions are associated to the solution of a linear system of the form $\boldsymbol{A}_s \boldsymbol{\mu}_s = \boldsymbol{b}_s$ that were solved using *simultaneous algebraic reconstruction technique method* (sart) provided by the MATLAB package IR Tools [8]. We observe that a stable reconstruction is possible in both cases but the lack of information in the limited-illumination case produces a gross reconstruction in the non-observable region.

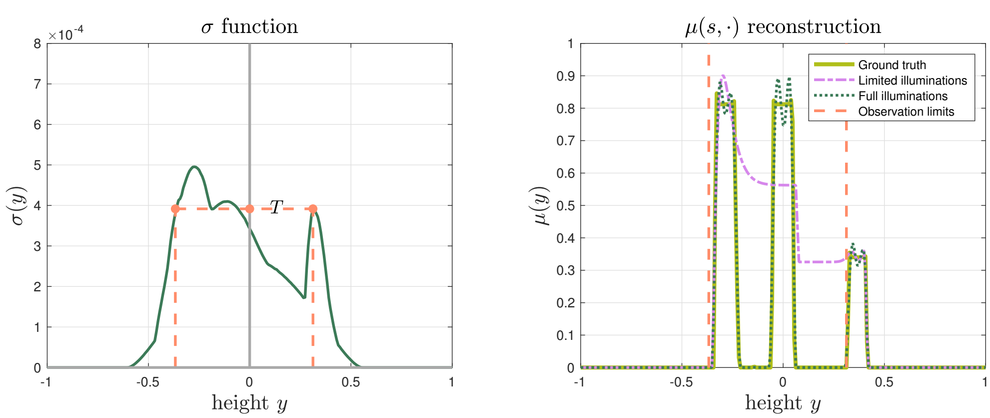

FIG. 13. *Reconstruction of $\mu(s,\cdot)$ for $s = 0.969$ using* `Dataset 3`. *On the left, σ function for the selected s with the corresponding observation interval whose limits are represented by a dashed line. On the right, $\mu(s,\cdot)$ and its limited and full reconstructions are added as profiles for ease of comparison.*

7. Conclusions. Two novel results has been established with respect to the stability for the reconstruction of the initial temperature for the heat equation in $\mathbb{R}^n$, for distinct domains of observation of the form $\omega \times (\tau, T)$. Typical results in the literature for the backward heat equation problem provide us with logarithmic estimates when incorporating some a priori information on the initial condition. In our case, we have been able to improve those estimates to a Lipschitz one, at least for compactly supported initial conditions. We expect that this result may be extended for more general initial temperatures. Furthermore, another interesting stability result is obtained for the reconstruction of the initial temperature for the heat equation in $\mathbb{R}$ when measurements are available on a curve $\Gamma \subset \mathbb{R} \times [0, \infty)$, a problem that arises from the LSFM model established in [6]. However, we have to be careful with these results, more specifically, we highlight the stability constant. Recall that this constant comes, in part, from the open mapping theorem, which ensure just the existence of this term, without giving any information about the dependency on the parameters of the problem. Consequently, if this constant is too large in comparison to the noise level in the measurements, then we can not expect a good reconstruction from the numerical point of view, despite the Lipschitz estimate. In fact, as numerical results indicate, even though a small noise is added to the measurements, the initial condition reconstructed is away from the real one in those sections where measurements are not taken into account, which give insights of a high value for the stability constant. We expect that the result may be improved by considering all the measurements available and not restricting to those heights of illumination for which σ is increasing or decreasing.

Acknowledgments. P.A. was partially funded by Basal Program CMM-AFB 170001 and Anid-Fondecyt grant #1191903. P.A. also thanks the Department of Mathematical Engineering at Universidad de Chile.
A.O. was partially funded by ANID-Fondecyt grants #1191903 and #1201311, Basal Program CMM-AFB 170001, FONDAP/15110009 and Millennium Nucleus for Cardiovascular Magnetic Resonance.
B.P. would like to thanks the Department of Mathematics at Pontificia Universidad Católica de Chile, for their hospitality during a visit in December 2018-January 2019.
M.C. was partially funded by Anid-Fondecyt grant #1191903.

REFERENCES

[1] R. Adams and J. Fournier, *Sobolev Spaces*, ISSN, Elsevier Science, 2003, https://books.google.cl/books?id=R5A65Koh-EoC.

[2] G. Bal, *Inverse transport theory and applications*, Inverse Problems, 25 (2009), p. 53001, https://doi.org/10.1088/0266-5611/25/5/053001, http://dx.doi.org/10.1088/0266-5611/25/5/053001.

[3] V. R. Cabanillas, S. B. de Menezes, and E. Zuazua, *Null controllability in unbounded domains for the semilinear heat equation with nonlinearities involving gradient terms*, Journal of Optimization Theory and Applications, 110 (2001), pp. 245–264.

[4] D. Chae, O. Y. Imanuvilov, and S. M. Kim, *Exact controllability for semilinear parabolic equations with neumann boundary conditions*, Journal of Dynamical and Control Systems, 2 (1996), p. 449–483, https://doi.org/10.1007/bf02254698, http://dx.doi.org/10.1007/bf02254698.

[5] S. N. Chandler-Wilde, D. P. Hewett, and A. Moiola, *Interpolation of Hilbert and Sobolev spaces: Quantitative estimates and counterexamples*, Mathematika, 61 (2014), p. 414–443, https://doi.org/10.1112/s0025579314000278, http://dx.doi.org/10.1112/S0025579314000278.

[6] E. Cueva, M. Courdurier, A. Osses, V. Castañeda, B. Palacios, and S. Härtel, *Mathematical modeling for 2d light–sheet fluorescence microscopy image reconstruction*, Inverse

Problems, (2020).
[7] C.-L. Fu, X.-T. Xiong, and Z. Qian, *Fourier regularization for a backward heat equation*, Journal of Mathematical Analysis and Applications, 331 (2007), p. 472–480, https://doi.org/10.1016/j.jmaa.2006.08.040, http://dx.doi.org/10.1016/j.jmaa.2006.08.040.
[8] S. Gazzola, P. C. Hansen, and J. G. Nagy, *Ir tools: a matlab package of iterative regularization methods and large-scale test problems*, Numerical Algorithms, 81 (2018), pp. 773–811, https://doi.org/10.1007/s11075-018-0570-7.
[9] J. M. Girkin and M. T. Carvalho, *The light-sheet microscopy revolution*, Journal of Optics, 20 (2018), p. 053002, https://doi.org/10.1088/2040-8986/aab58a, https://doi.org/10.1088%2F2040-8986%2Faab58a.
[10] J. Hadamard and P. M. Morse, *Lectures on cauchy's problem in linear partial differential equations*, Physics Today, 6 (1953), p. 18–18, https://doi.org/10.1063/1.3061337, http://dx.doi.org/10.1063/1.3061337.
[11] J. Huisken and D. Y. R. Stainier, *Selective plane illumination microscopy techniques in developmental biology*, Development, 136 (2009), p. 1963–1975, https://doi.org/10.1242/dev.022426, http://dx.doi.org/10.1242/dev.022426.
[12] D. N. Hào and N. V. Duc, *Stability results for the heat equation backward in time*, Journal of Mathematical Analysis and Applications, 353 (2009), p. 627–641, https://doi.org/10.1016/j.jmaa.2008.12.018, http://dx.doi.org/10.1016/j.jmaa.2008.12.018.
[13] O. Y. Imanuvilov and M. Yamamoto, *Carleman inequalities for parabolic equations in sobolev spaces of negative order and exact controllability for semilinear parabolic equations*, Publications of the Research Institute for Mathematical Sciences, 39 (2003), pp. 227–274.
[14] J. Lakowicz, *Principles of Fluorescence Spectroscopy*, Springer US, 2006, https://doi.org/10.1007/978-0-387-46312-4, http://dx.doi.org/10.1007/978-0-387-46312-4.
[15] J. Li, M. Yamamoto, and J. Zou, *Conditional stability and numerical reconstruction of initial temperature*, Communications on Pure and Applied Analysis, 8 (2009), pp. 361–382, https://doi.org/10.3934/cpaa.2009.8.361.
[16] J. L. Lions and E. Magenes, *Non-Homogeneous Boundary Value Problems and Applications*, Springer Berlin Heidelberg, 1972, https://doi.org/10.1007/978-3-642-65161-8, http://dx.doi.org/10.1007/978-3-642-65161-8.
[17] S. Micu, *On the lack of null-controllability of the heat equation on the half-line*, Transactions of the American Mathematical Society, 353 (2001), https://doi.org/10.2307/221872.
[18] S. Micu and E. Zuazua, *On the lack of null-controllability of the heat equation on the half space*, Portugaliae Mathematica, 58 (2001).
[19] E. D. Nezza, G. Palatucci, and E. Valdinoci, *Hitchhiker's guide to the fractional sobolev spaces*, 2011, https://arxiv.org/abs/1104.4345.
[20] S. Saitoh and M. Yamamoto, *Stability of lipschitz type in determination of initial heat distribution*, Journal of Inequalities and Applications, 1997 (1997), p. 219593, https://doi.org/10.1155/s1025583497000052, http://dx.doi.org/10.1155/S1025583497000052.
[21] M. E. Taylor, *Partial Differential Equations I*, Springer New York, 2011, https://doi.org/10.1007/978-1-4419-7055-8, https://doi.org/10.1007/978-1-4419-7055-8.
[22] H. Triebel, *Interpolation Theory, Function Spaces, Differential Operators*, Huthig Pub Limited, 1995, https://books.google.cl/books?id=ZzvvAAAAMAAJ.
[23] T. M. N. Vo, *The local backward heat problem*, 2017, https://arxiv.org/abs/1704.05314.
[24] D. Xu and M. Yamamoto, *Stability Estimates in State-Estimation for a Heat Process*, Springer US, 2000, p. 193–198, https://doi.org/10.1007/978-1-4613-0269-8_25, http://dx.doi.org/10.1007/978-1-4613-0269-8_25.